Solar Phys
DOI 10.1007/s11207-016-0946-6

Interplanetary Type IV Bursts

A. Hillaris[1] · **C. Bouratzis**[1] · **A. Nindos**[2]

Received: 21 December 2015 / Accepted: 21 June 2016

Abstract We study the characteristics of moving type IV radio bursts that extend to hectometric wavelengths (interplanetary type IV or type IV_{IP} bursts) and their relationship with energetic phenomena on the Sun. Our dataset comprises 48 interplanetary type IV bursts observed with the *Radio and Plasma Wave Investigation* (WAVES) instrument onboard *Wind* in the 13.825 MHz – 20 kHz frequency range. The dynamic spectra of the *Radio Solar Telescope Network* (RSTN), the *Nançay Decametric Array* (DAM), the *Appareil de Routine pour le Traitement et l' Enregistrement Magnetique de l' Information Spectral* (ARTEMIS-IV), the *Culgoora*, *Hiraso*, and the *Institute of Terrestrial Magnetism, Ionosphere and Radio Wave Propagation* (IZMIRAN) *Radio Spectrographs* were used to track the evolution of the events in the low corona. These were supplemented with soft X-ray (SXR) flux-measurements from the *Geostationary Operational Environmental Satellite* (GOES) and coronal mass ejections (CME) data from the *Large Angle and Spectroscopic Coronagraph* (LASCO) onboard the *Solar and Heliospheric Observatory* (SOHO). Positional information of the coronal bursts was obtained by the *Nançay Radioheliograph* (NRH). We examined the relationship of the type IV events with coronal radio bursts, CMEs, and SXR flares. The majority of the events (45) were characterized as compact, their duration was on average 106 minutes. This type of events was, mostly, associated with M- and X-class flares (40 out of 45) and fast CMEs, 32 of these events had CMEs faster than

Electronic supplementary material The online version of this article (doi:10.1007/s11207-016-0946-6) contains supplementary material, which is available to authorized users.

✉ A. Hillaris
ahilaris@phys.uoa.gr

C. Bouratzis
kbouratz@phys.uoa.gr

A. Nindos
anindos@cc.uoi.gr

1 Section of Astronomy, Astrophysics and Mechanics, Department of Physics, University of Athens, 15783 Athens, Greece

2 Section of Astro-geophysics, Department of Physics, University of Ioannina, 45110 Ioannina, Greece

Published online: 18 July 2016

1000 $\mathrm{km\,s^{-1}}$. Furthermore, in 43 compact events the CME was possibly subjected to reduced aerodynamic drag as it was propagating in the wake of a previous CME. A minority (three) of long-lived type $\mathrm{IV_{IP}}$ bursts was detected, with durations from 960 minutes to 115 hours. These events are referred to as extended or long duration and appear to replenish their energetic electron content, possibly from electrons escaping from the corresponding coronal type IV bursts. The latter were found to persist on the disk, for tens of hours to days. Prominent among them was the unusual interplanetary type IV burst of 18 – 23 May 2002, which is the longest event in the *Wind*/WAVES catalog. The three extended events were typically accompanied by a number of flares, of GOES class C in their majority, and of CMEs, many of which were slow and narrow.

Keywords Radio bursts · Dynamic spectrum · Meter and longer wavelengths · Coronal mass ejections

1. Introduction

Solar metric radio bursts provide a unique diagnostic of the development of flare events accompanied by coronal mass ejections (CME) in the low corona, flare-CME events from now on. Their onset and evolution is accompanied by energetic-particle acceleration and injection into interplanetary (IP) space as well as shocks (see *e.g.* the review by Pick and Vilmer, 2008; Nindos *et al.*, 2008). Their signatures at metric to kilometric wavelengths trace disturbances propagating from the low corona to the interplanetary space.

Three types of nonthermal radio bursts are associated with the flare-CME events (Sakurai, 1974; White, 2007; Gopalswamy, 2011):

- Bursts of the type III family. They are produced by energetic electrons accelerated in the Sun and traversing the solar atmosphere, along coronal magnetic lines rooted in its surface. In open field lines, they may escape into the interplanetary space (see, for example, Figure 1 of Klein *et al.*, 2008, also Alissandrakis *et al.*, 2015). In the dynamic spectra, these standard type III bursts appear as fast-drifting bands ($\mathrm{d}f/f\,\mathrm{d}t \approx 1.0\ \mathrm{s^{-1}}$). When trapped in closed magnetic structures, they eventually turn toward the Sun, resulting in inverted U- or J-shaped bursts in the dynamic spectra (hence U- or J-type bursts of the type III family). In flare-CME events, the transition from the type U and J bursts to the typical type III often marks the restructuring, or opening, of the magnetic field lines as originally confined, energetic electrons gain access to open magnetic lines. An example of dynamic radio spectra showing this transition from U- and J-type bursts to a standard type III burst at the beginning of the 17 January 2005 event can be found in Hillaris *et al.* (2011). In the hectometric and kilometric regime, long-duration storms of individual type III bursts (Fainberg and Stone, 1970a,b, 1971; Bougeret, Fainberg, and Stone, 1983) covering several days (5.4 on average according to Kayser *et al.*, 1987) were recorded. These are different from the hectometric–kilometric extensions of type III bursts and are known as IP storms and, more often than not, may appear as storm continua on the dynamic spectra. The individual type III components of the IP storms (micro-type III bursts, according to Morioka *et al.*, 2007) are significantly weaker than the typical type III bursts in the same frequency range. The IP storms are well associated with active regions (Kayser *et al.*, 1987), but the micro-type III bursts are not accompanied by significant soft X-ray (SXR) flare activity. This implies the need of a persistent coronal store of suprathermal electrons (Bougeret, Fainberg, and Stone, 1984a,b) supplying this type of activity.

- Type II bursts. They are the radio signatures of the passage of a magneto-hydrodynamic (MHD) shock wave through the tenuous plasma of the solar corona; their radio emission is due to energetic electrons accelerated at the shock front. It is in general accepted that type II bursts at decametric and longer wavelengths are driven by CME bows or flanks (Vršnak and Cliver, 2008). At the metric range, on the other hand, they might be also due to flare blasts, in addition to CMEs (Cane and Reames, 1988; Nindos *et al.*, 2011; Magdalenić *et al.*, 2010, 2012), or to reconnection outflow termination-shocks (Aurass, Vršnak, and Mann, 2002).
- Type IV bursts. They are radio continua caused by the radiation of energetic electrons trapped within magnetic structures and plasmoids. They have been recorded in almost all frequency ranges starting from the microwaves as type IVμ bursts and the decimetric range as type IVdm bursts (Benz, 1980). In the metric wavelengths the type IVm bursts are divided into moving (IVmA or IVM) and stationary (IVmB). The type IVmB bursts emanate from stationary magnetic structures that are typically located above active regions or post-eruption arcades behind CMEs (Robinson, 1985; Gopalswamy, 2011). The type IVm burst are sometimes referenced as flare continua (FCM when preceding a type IVmA or FCII when following a type II burst, see Robinson, 1978). They are also identified as continuum noise storms (type IVsA and IVsB, corresponding to type IVmA and IVmB, see discussion in Sakurai, 1974, and their Figure 14). The type IVmA bursts (Boischot, 1957) appear to be moving outward at velocities of about $100-1000\ \mathrm{km\,s^{-1}}$, which are comparable to CME speeds (White, 2007); they sometimes last more than ten minutes. A number of these are believed to originate within the densest substructures of CMEs (Klein and Mouradian, 2002; Bastian *et al.*, 2001; Aurass *et al.*, 1999; Bain *et al.*, 2014). These substructures might be erupting prominences within the CMEs. The type IVmA burst – CME association was found to increase with the speed of the CME (Gergely, 1986, and references therein). A subset of the moving type IV radio bursts extend in dynamic spectra to the hectometric wavelengths (frequencies lower than ≈ 20 MHz) and are recorded with the *Radio and Plasma Wave Investigation* (WAVES) instrument onboard *Wind*; these are interplanetary type IV or $\mathrm{IV_{IP}}$ radio bursts.

In this article we examine the characteristics and the evolution of interplanetary type IV bursts and their relationship with energetic phenomena on the Sun such as flares and CMEs. The data used are from the *Wind*/WAVES receivers and a number of ground-based instruments. From the combined datasets an extensive table of type $\mathrm{IV_{IP}}$ and associated activity was compiled and is presented as supplementary online material (file IPtypeIV.pdf). A detailed description of the table is included in the Appendix. The question addressed in our study is twofold. First, we examine the association of these bursts with intense flares and fast CMEs, examining whether they may be considered as another aspect of the big flare syndrome first introduced by Kahler (1982). Second, we search for other processes affecting, totally or partially, the appearance of this type of radio bursts.

This report on interplanetary type IV (or type $\mathrm{IV_{IP}}$) bursts is structured as follows. In Section 2 we describe the instrumentation and datasets used in our study. The data analysis is presented in Section 3, including an overview of selected events in Sections 3.3, 3.4, and 3.5. In Section 4 we present the characteristics and the evolution of different types of type $\mathrm{IV_{IP}}$ events, which are then discussed in Section 5. The conclusions are presented in the same section.

2. Observations and Data Selection

The basic data used in this study are dynamic spectra recorded by the R1 and R2 receivers of the *Wind*/WAVES (Bougeret *et al.*, 1995) in the 20 kHz – 13.825 MHz frequency range from 1998 to 2012. The interplanetary type IV bursts selected were previously identified in the *Wind*/WAVES online catalog.[1] The observations were complemented by data in the metric and decametric wavelengths from the following ground-based radio observatories:

- The ARTEMIS-IV[2] radio spectrograph (Caroubalos *et al.*, 2001; Kontogeorgos *et al.*, 2006a,b, 2008) observes in the frequency range 20 – 650 MHz.
- The *Culgoora Radio Spectrograph* (Prestage *et al.*, 1994) observes in the frequency range 18 – 1800 MHz.
- The *Nançay Decametric Array*[3] (DAM: Boischot *et al.*, 1980; Lecacheux, 2000) observes in the range 20 – 75 MHz.
- *The Nançay Radioheliograph* (NRH: Kerdraon and Delouis, 1997) provides daily, 09:00 – 15:30 UT, two-dimensional images of the Sun at ten frequencies from 450 to 150 MHz with sub-second time resolution. It was used for positional information of the metric–decametric radio emission. In this article the quick-look-style NRH data from the radio-monitoring site[4] were used.
- The *Hiraiso Radio Spectrograph*[5] (HiRAS: Kondo *et al.*, 1995) observes in the frequency range 25 – 2500 MHz.
- *The Institute of Terrestrial Magnetism, Ionosphere and Radio Wave Propagation* (IZMIRAN) *Radio Spectrograph*[6] (Gorgutsa *et al.*, 2001) observes in the range 25 – 270 MHz.
- *The Radio Solar Telescope Network*[7] (RSTN: Guidice *et al.*, 1981) with a number of solar radio observatories at various locations around the world guarantees full 24-hour coverage:
  - Sagamore Hill at Hamilton, Massachusetts, USA (42°33′N 70°49′W);
  - Palehua at Kaena Point, Hawaii (21°24′N 158°06′W);
  - Holloman at New Mexico, USA (32°51′N 106°06′W);
  - Learmonth at Western Australia, Australia (22°13′S – 114°06′E);
  - San Vito dei Normanni, Italy (40°39′N 17°42′E).

  These observatories provide dynamic spectra in the 25 – 180 MHz range.

Additional datasets were used to examine the association of the type IV_{IP} bursts with the evolution of flares and CMEs:

- CME data from the *Large Angle and Spectroscopic Coronagraph* (LASCO) Catalog online[8] (Yashiro *et al.*, 2004; Gopalswamy *et al.*, 2009).

[1] www.lep.gsfc.nasa.gov/waves/data_products.html.

[2] *Appareil de Routine pour le Traitement et l' Enregistrement Magnetique de l' Information Spectral*, http://artemis-iv.phys.uoa.gr/.

[3] bass2000.obspm.fr/home.php.

[4] http://radio-monitoring.obspm.fr/nrh_data.php.

[5] sunbase.nict.go.jp/solar/denpa/index.html.

[6] www.izmiran.ru/stp/lars/.

[7] ftp://ftp.ngdc.noaa.gov/STP/space-weather/solar-data/solar-features/solar-radio/rstn-spectral.

[8] http://cdaw.gsfc.nasa.gov/CME_list.

- SXR characteristics such as online reports[9] and light curves[10] from the *Geostationary Operational Environmental Satellite* (GOES).
- Images from the *Extreme Ultraviolet Imaging Telescope* (EIT: Delaboudinière *et al.*, 1995) onboard the *Solar and Heliospheric Observatory* SOHO. They were used to provide information on flare positions.

From the *Wind*/WAVES catalog all events indicated as bursts of type IV_{IP} (48 in total) were selected. Many (36) were accompanied by interplanetary type II shocks.

A comprehensive list of the interplanetary type IV bursts and the associated activity including, but not restricted to, coronal burst, flare, and CME characteristics is attached as supplementary online material (file IPtypeIV.pdf). A detailed description of the table is included in the Appendix. In compiling this catalog, we included information of all the *Wind*/WAVES type IV_{IP} bursts, their associated CMEs and SXR flares in the 1998 – 2012 period, and the accompanying interplanetary type II and coronal type II, IV, and III bursts. The above-mentioned CMEs that are thought to drive the type IV_{IP} bursts are referred to as main CMEs to distinguish them from preceding CMEs along the same path; the latter were included in the table as they may affect the appearance of type IV_{IP} bursts, as discussed in Sections 4.1 and 5. The selection of the CMEs preceding the main ejection along the same path is based on a time interval of about 48 hours before the main CME and whether the sectors (or cones in 3D) defined by position angle and width for the main and the preceding CME overlap. Occasionally, more than one preceding CME is included in the catalog because they are all within the 48 hours window and appear to overlap in part with the main CME. The overlap criterion is relaxed when one or both the main and the preceding CMEs are halo CMEs; in this case we assume that an overlap is always possible, at least in part.

3. Data Analysis

3.1. Data Processing

The combination of hectometric dynamic spectra by *Wind*/WAVES with metric and decametric spectra from the ground-based radio spectrographs (see Section 2) was first plotted as a composite dynamic spectrum. These were found to include an amount of features, mostly groups of type III and II bursts, embedded in a slowly varying background. Often the continuum background was removed by the use of differentiation of the dynamic spectra in time domain. This filtering, however, amplifies the high-frequency noises, therefore the smoothed differentiation filter of Usui and Amidror (1982) was used. This simultaneously performs a smoothing and differentiation, so that it can be regarded as a low-pass differentiation filter (digital differentiator) appropriate for experimental (noisy) data processing.

The composite dynamic spectra provide an overview of the evolution of the type IV_{IP} bursts under study and of the accompanying radio activity, from the corona to the interplanetary space. On each dynamic spectrum several time-histories were superposed:

- The approximate frequency–time trajectories of the CME fronts. These were plotted on the dynamic spectra, using the coronal density model of Vršnak, Magdalenić, and Zlobec (2004), as thick-dotted lines. The details of the model are presented in Section 3.2. The linear fits to the height–time trajectories of the CME fronts, from the LASCO images,

[9] ftp://ftp.ngdc.noaa.gov/STP/space-weather/solar-data/solar-features/solar-flares/x-rays/ and https://solarmonitor.org/data.

[10] http://satdat.ngdc.noaa.gov/sem/goes/data/.

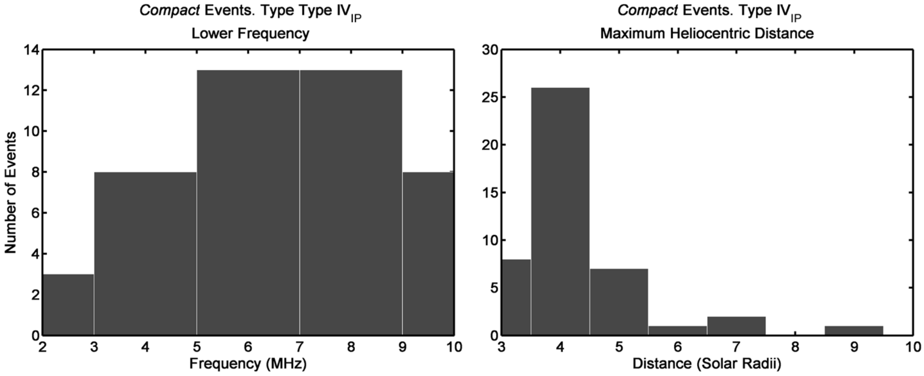

Figure 1 Left panel: distribution of the low-frequency limit of the compact interplanetary type IV bursts. Right panel: the corresponding heliocentric distance of these type IV bursts based on the low-frequency limit and the model dependent calculations described in Section 3.2.

were converted into the frequency–time traces of the fundamental and harmonic plasma emission; the squares mark the measured positions of the CME front.

- The GOES SXR time-profiles. The solid black (1.0 – 8.0 Å) and the thick-dotted magenta (0.5 – 4.0 Å) curves display the SXR time history describing thermal emission from the hot flare plasma.

Of the 48 type IV_{IP} bursts in this article, 17 overlapped at least partly with the NRH window of observation. For these, the position of the coronal extension (metric type IV burst) of the interplanetary burst was compared to the SXR flare position and the solar sources of the CME in the EIT images. Their spatial relationship was established combining NRH radio contours overlayed on the EIT 195 Å difference image and LASCO difference image. Two categories of type IV_{IP} bursts were found:

Compact type IV_{IP} bursts. These were mostly associated with M- and X-class flares and fast CMEs; their duration was on average 100 (±11) minutes. Their minimum frequency was in the 10 – 2 MHz range, which corresponds to 3 – 10 $R_{\odot}$ heliocentric distances. The distribution of the low-frequency limits and the corresponding distances, derived from the calculations in Section 3.2, are exhibited in Figure 1. In total, 45 of these events were found in the *Wind*/WAVES lists. An example is presented in Section 3.3.

Long-duration or extended type IV_{IP} bursts. They represent a small minority of three events with durations from 960 minutes to 115 hours. Their morphology was found to be less uniform than that of their counterparts. Two of them (catalog numbers 34, 18 – 23 May 2002, and 45, 27 May 1999, described in Sections 3.4 and 3.5) were accompanied by a sequence of small flares and slow and narrow CMEs with an occasional medium or large flare within the sequence. Another event (number 14, 17 January 2005, presented in Section 3.6) originated from a fast CME and large flare, but extended far beyond the duration of a compact event.

The distribution of the interplanetary type IV bursts duration is presented in Figure 2 for all the events of the study. The three extended events are the outliers of the histogram in the left panel. The distribution of the duration of the compact events is also presented separately in the right panel of Figure 2. In Section 4 the differences between the characteristics of the extended and the compact events are examined and discussed, except for their duration.

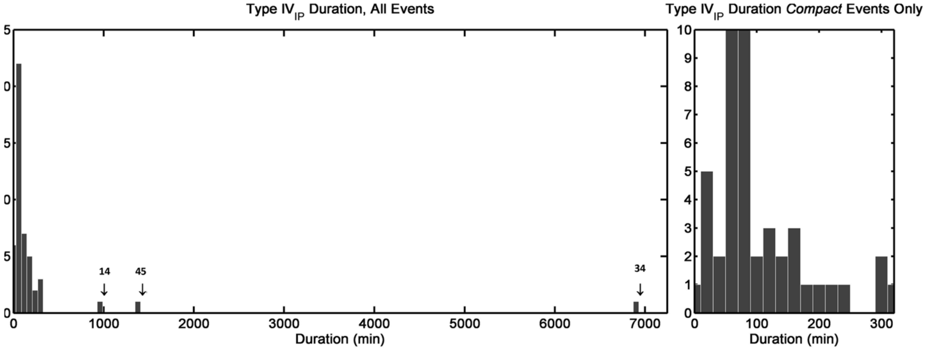

Figure 2 Distribution of the duration of the interplanetary type IV bursts. Left panel: all (48) events; the three extended events are pointed with arrows. Their catalog numbers are shown above them. Right panel: histogram including only the 45 compact events.

3.2. Coronal Density-Height Model Selection

As plasma emission depends on the electron density, which in turn may be converted into a coronal height using density models, we may calculate the radio source heights and speeds from the dynamic spectra. The establishment of a correspondence between frequency of observation-coronal height and frequency drift rate-radial speed is affected by ambiguities introduced by the variation of the ambient medium properties. These may be the result of the burst exciter propagation in the undisturbed plasma, overdense or underdense structure or CME afterflows (see Pohjolainen *et al.*, 2007; Pohjolainen, Hori, and Sakurai, 2008, for a detailed discussion on model selection).

The density model of Vršnak, Magdalenić, and Zlobec (2004),

$$\frac{n}{10^8\ \mathrm{cm}^{-3}} = 15.45\left(\frac{R_\odot}{R}\right)^{16} + 3.165\left(\frac{R_\odot}{R}\right)^{6} + 1.0\left(\frac{R_\odot}{R}\right)^{4} + 0.0033\left(\frac{R_\odot}{R}\right)^{2},$$

which describes the coronal density behavior well in the wide range of distances from the low corona to interplanetary space was used to convert the linear fits to the height–time trajectories of the LASCO CME fronts to frequency–time tracks on the composite dynamic spectra.

3.3. Overview of the 2 May 1998 Compact Event Evolution

The 2 May 1998 compact event (catalog number 47) is typical of its class. It has drawn considerable attention due to the large number of instruments that have observed it, including *Wind*/WAVES, LASCO, EIT, NRH, and several radio spectrographs. It is reported in a number of articles that mainly focused on the solar surface magnetic waves (Zharkova and Kosovichev, 1999), the pre-CME launch activity (Pohjolainen, Khan, and Vilmer, 1999), and the on-disk development of the CME (Pohjolainen *et al.*, 2001).

The interplanetary type IV event (see composite spectrum in Figure 3) starts at 14:10 UT on 02 May and lasts until 15:40 UT of the same day in the frequency range 8 – 14 MHz. An interplanetary type II burst was recorded from 14:25 – 14:50 UT in the 3 – 5 MHz range of *Wind*/WAVES. In the catalog it is described as a narrowband wisp, but it is well associated

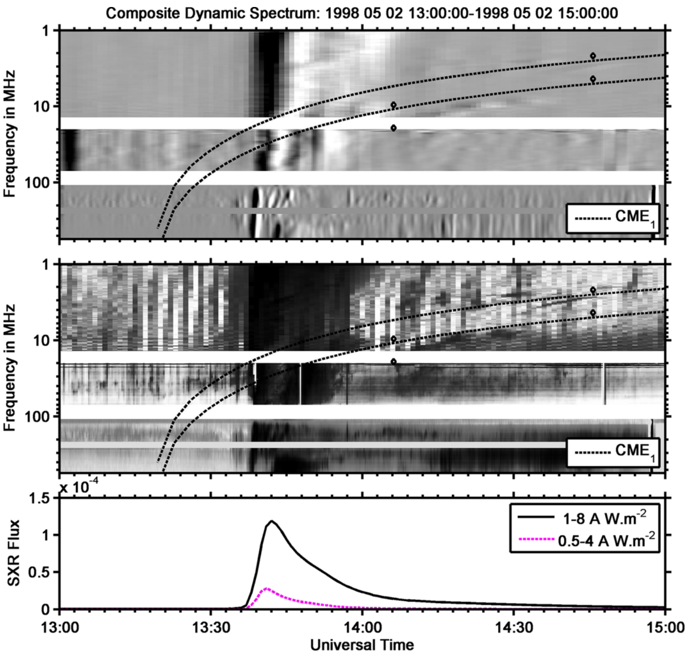

Figure 3 02 May 1998 event. Top panel: *Wind*/WAVES and ARTEMIS-IV differential spectrum (inverse grayscale). Middle panel: dynamic (intensity, inverse grayscale) spectrum. The frequency–time plots derived from the linear fit to the front trajectory of the associated CME and an empirical density model (see Section 3.2) for the fundamental and harmonic (thick-dotted curves) plasma emission are overlaid on the spectra. Bottom panel: the profiles of GOES SXR 1 – 8 Å (solid black line) and 0.5 – 4 Å (thick-dotted magenta line) flux.

with the front of the CME. Another type II, without apparent association with the CME front, appears in the 6 – 400 MHz range, recorded by the ARTEMIS-IV, the *Nançay Decametric Array* (DAM), and the *Wind*/WAVES from 13:30 – 13:46 UT. The event exhibits a multiple band structure and was first reported by Pohjolainen *et al.* (2001). The high-frequency extension of the type IV_{IP} was recorded by the DAM and the ARTEMIS-IV radio spectrographs and extended above the 500 MHz (see also Pohjolainen *et al.*, 2001, their Figure 8). This activity is accompanied by an X1.1/3B-class flare from active region (AR) 8210 at heliographic coordinates S15W15; the flare started at 13:31 and ended at 13:51 UT, peaking at 13:42 UT.

The NRH records at 432 and 164 MHz indicate that the type IV continuum appeared over AR 8210 and, in the 164 MHz images, started moving northward at 13:34 UT. This is consistent with the motion of a rather fast, 938 $\mathrm{km\,s^{-1}}$, halo CME (first viewed at 14:06 UT, back-extrapolated lift-off at 13:07 UT) with measured position angle 331° (see Figure 4). This CME appears to drive the fundamental and harmonic pair mentioned in the previous paragraph. As regards the CME path, there were two preceding halo CMEs on 02 May 1998 at 05:32 UT and on 01 May 1998 at 23:40 UT.

The broadband dynamic spectra and the NRH images indicate that the compact interplanetary type IV burst is associated with an X-class flare and the fast halo-CME. The latter propagates in the wake of a previous halo-CME that was launched approximately 8.5 hours before. This example represents the combined effects of an intense flare and a fast CME with the CME propagating within a low-drag region due to the passage of a previous CME.

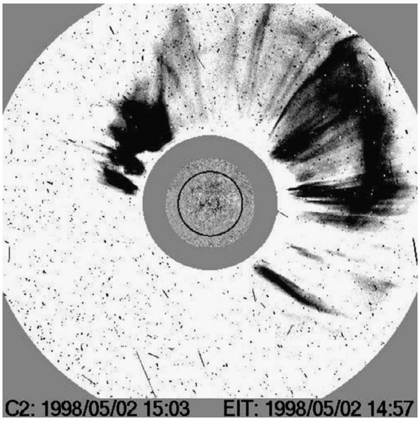

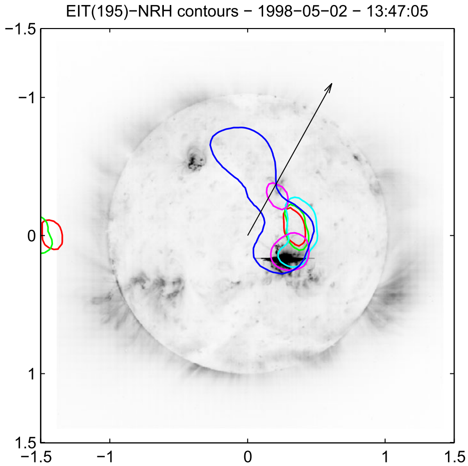

Figure 4 Left: LASCO and EIT 195 Å running-difference frames of the 02 May 1998 14:06 UT CME (inverse grayscale). Right: NRH half-power contours (at 432 (red), 410 (green), 327 (cyan), 236 (magenta), and 164 (blue) MHz). The contours were recorded at successive times starting with 432 MHz at 13:47:05 UT to 164 MHz at 13:51:53 UT, thus tracing the outward motion of the type IV burst. The arrow indicates the halo-CME measured position angle from the LASCO catalog.

3.4. Overview of the 18 – 22 May 2002 Extended Event Evolution

The type IV_{IP} event started at 09:00 UT on 18 May and lasted until 04:00 UT on 23 May in the frequency range 0.3 – 9 MHz (catalog number 34). It was the only such event observed by *Wind*/WAVES in its years of operation (Reiner *et al.*, 2006). An interplanetary type II burst was recorded from 22 May at 04:10 UT until 23 May 10:10 UT in the 0.03 – 0.5 MHz range. The *Wind*/WAVES dynamic and differential spectra, with the CME front trajectories overlaid, and the SXR flux are exhibited in Figure 5; details in the period 07:45 – 12:45 UT on 19 May are presented in Figure 6. This event was briefly reported by Gopalswamy (2004), who, based on polarization measurements, considered it as a hectometric storm continuum and not a type IV_{IP} burst, as reported in the *Wind*/WAVES catalog.

On the solar disk, we see a number of active-region complexes in the 18 – 23 May period. When the continuum emission started, on 18 May AR 9957 (N08E47) was the largest and most complex region on the disk. This region was accompanied by AR 9958 (N04E45) and followed by AR 9960 at N05E74 and AR 9962 and AR 9963, which appeared on 21 May at N15E47 and N17E63, respectively. South of this group were AR 9954 (S22E35), AR 9955 (S14E37), and in the western hemisphere AR 9945 (S02W73), AR 9948 (S21W20), and AR 9950 (S05W42). In the left panel of Figure 7 we present the positions of all SXR flares within the 18 – 23 period and of the corresponding active regions.

Throughout the period of interest from 18 May 2002 at 02:44 UT to 23 May 2002 at 04:00 UT, 38 SXR flares were recorded by GOES; positional data were obtained for 33 of them. The AR 9957, AR 9958, AR 9960, AR 9962, and AR 9963 complex, located in the NE quadrant of the disk, produced 10 C-class and one M1.5 SXR flares. The single AR 9961 in the SE quadrant produced 16 flares (including an X2.1 and an M5.0) on 19 May 2002 at 15:54 UT. Within the same period, 24 CMEs were recorded in the LASCO catalog. The position angles, shown in the right panel of Figure 7, indicate that they emerged from all quadrants of the solar disk. This activity was associated with many type III burst-groups,

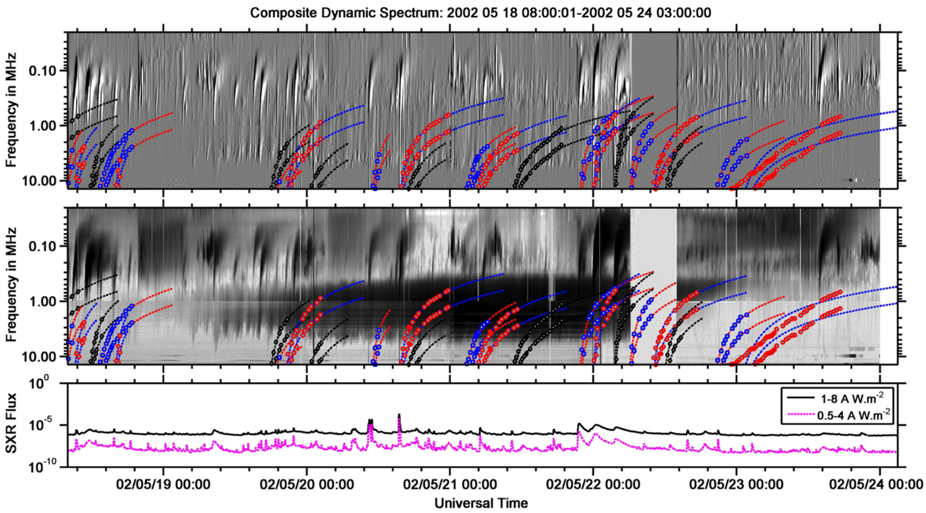

Figure 5 18 – 22 May 2002 event (18:08:00 UT on 18 May to 00:03:00 UT on 23 May). Top panel: *Wind*/WAVES differential spectrum (inverse grayscale). Middle panel: dynamic (intensity, inverse grayscale) spectrum. The frequency–time plots derived from the linear fits to the front trajectory of the associated CMEs and the density model presented in Section 3.2 for the fundamental and harmonic (thick-dotted curves) plasma emission are overlaid on the spectra. In this example, the CME trajectories are shown with different colors. The squares that mark the positions of the CME fronts are drawn in black on the black trajectories, in red on the blue trajectories, and in blue on the red trajectories (see Section 3.1). Bottom panel: the profiles of GOES SXR 1 – 8 Å (solid black line) and 0.5 – 4 Å (thick-dotted magenta line) flux. The time is written in the format date, hours, and minutes.

2 – 3 type II shocks in the metric range (see the table included as supplementary online material), and a persistent continuum appearing in the NE quadrant over the AR 9957, AR 9958, AR 9960, AR 9962, and AR 9963 group during the 19 – 23 May period. The metric and decametric continuum appears in the SW quadrant, over AR 9948, only on 18 May (see Figure 8); on this day, it coexisted with the persistent continuum (over the AR 9957) mentioned above.

The SXR activity originates mostly in the NE (AR 9957, AR 9958, AR 9960, AR 9962, and AR 9963) and the SE (AR 9961) quadrants; most of the CME position angles indicate ejections from the same two quadrants (see Figure 7, right panel). The position of the type III bursts that could be localized were almost equally divided between the SE and NE quadrants, but the vast majority clearly appears to continue into the *Wind*/WAVES hectometric range in the differential spectra at frequencies lower than those of the type IV_{IP}. Furthermore, the type III and CME activity continues past the end of the interplanetary type IV burst. The metric continuum, on the other hand, appears persistently in the NRH images on top of the group formed by AR 9957, AR 9958, AR9960, AR 9962, and AR 9963 from 19 to 23 May. This implies a steady coronal reservoir of energetic electrons, which may follow the magnetic lines trailing CMEs originating at the NE quadrant and replenish the electrons of the interplanetary type IV_{IP} burst.

3.5. Overview of the 27 – 28 May 1999 Extended Event Evolution

The event started on 27 May 1999 at 10:55 UT and ended on 28 May at 15:00 UT (catalog number 45). The event was composed of interplanetary type II/IV bursts having both coro-

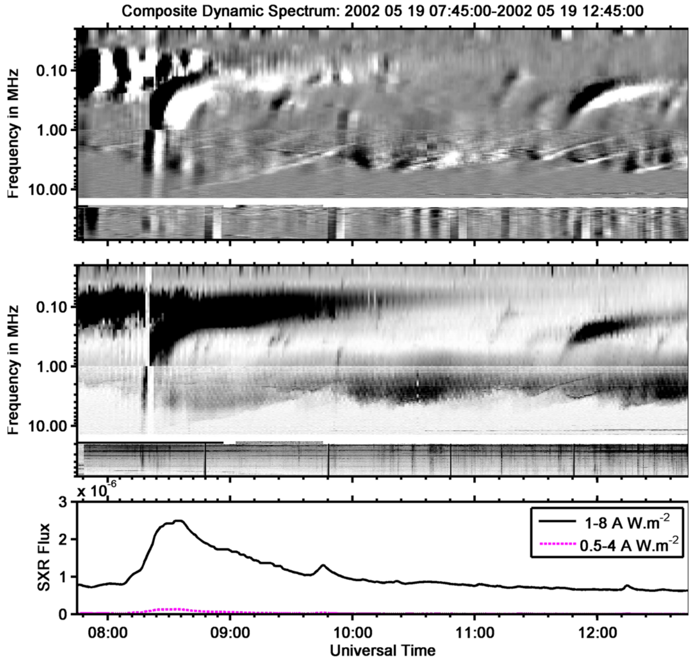

Figure 6 18 – 22 May 2002 event showing details on 19 May from 07:45 UT to 12:45 UT. The dynamic spectra are combined records from *Wind*/WAVES and DAM, extended in the 0.02 – 70 MHz range. Top panel: differential spectrum (inverse grayscale). Middle panel: dynamic (intensity, inverse grayscale) spectrum. Bottom panel: the profiles of GOES SXR 1 – 8 Å (solid black line) and 0.5 – 4 Å (thick-dotted magenta line) flux.

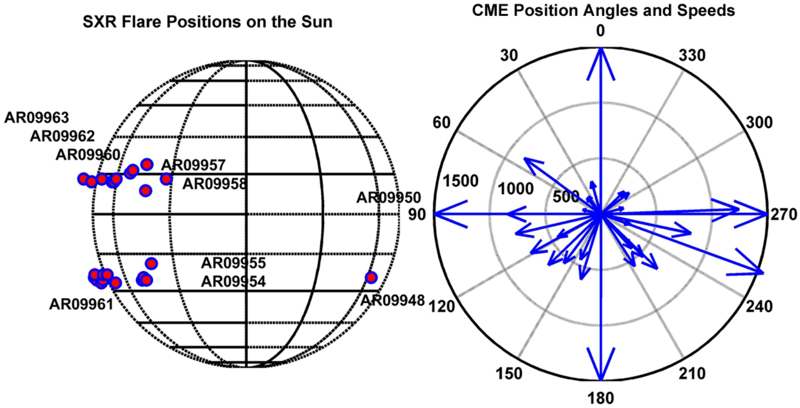

Figure 7 Left: Positions of the SXR flares (purple dots with blue border) and active regions. The AR positions, indicated approximately by their names, are taken from the SolarMonitor (http://www.solarmonitor.org) on 20 May 2002. Right: CME position angles and speeds indicated with segments ending in an arrowhead. The segment length is proportional to the CME speed. The flare and CME positions extend throughout the whole 18 – 23 May 2002 period.

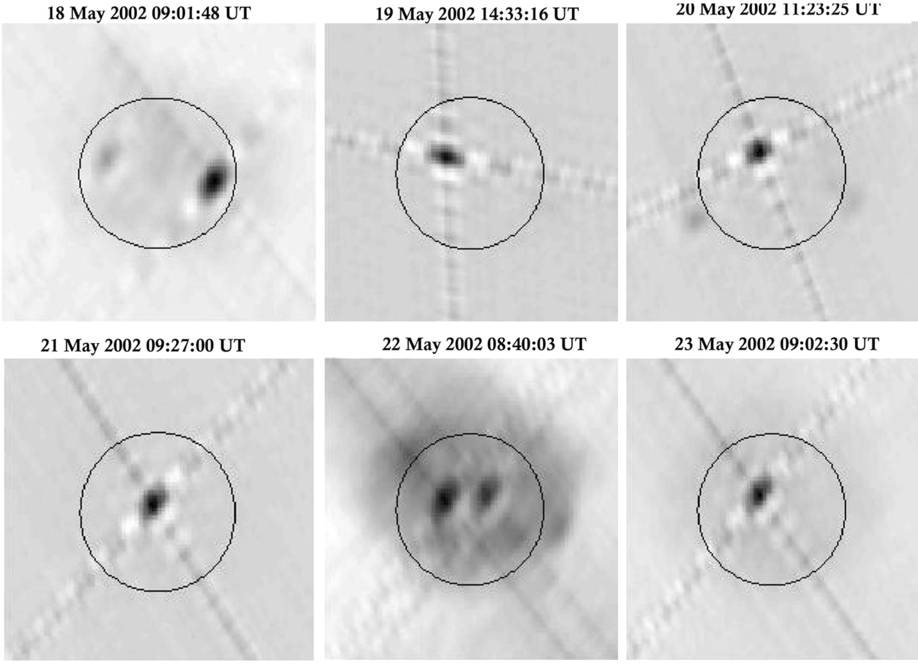

Figure 8 Positions of the coronal type IV bursts in the 18 – 23 May 2002 period, obtained with the *Nançay Radioheliograph* at 164 MHz.

nal extensions. This event was accompanied by a number of C-class SXR flares and narrow CMEs. An overview including the *Wind*/WAVES dynamic spectrum, the CME front trajectories, and the SXR flux profiles is presented in Figure 9. There are only two wide CMEs, a halo CME on 27 May at 11:06 UT and a rather wide CME on 28 May at 10:26 UT, which almost mark the start and the end of the event. Figures 10 and 11 show details of this event in different time periods on 27 and 28 May.

Similar to the 18 – 22 May 2002 event, in Section 3.4, there was also a persistent coronal type IV burst, which appeared over AR 8552 (N18E31) in the NRH records. This region remained active throughout the duration of the interplanetary type IV burst, and most of the small SXR flares and a number of type III bursts originated from it as well. In Figure 12 we present the position of the coronal type IV burst on 27 and 28 May in NRH images. There is also a long series of type III bursts and groups that covers the type $\mathrm{IV_{IP}}$ interval. Most of these type III bursts, however, overshoot the type $\mathrm{IV_{IP}}$ continuum, so that we expect that the main source of energetic electrons is its coronal counterpart persisting over AR8552.

3.6. Overview of the 17 January 2005 Extended Event Evolution

On 17 January 2005, two fast CMEs were recorded in close succession during two distinct episodes of a 3B/X3.8 flare in AR 10720. The type $\mathrm{IV_{IP}}$ burst started at 10:55 UT on 17 January and ended on 18 January at 02:00 UT (event catalog number 14); for an overview of the dynamic spectrum see Figure 3 of Hillaris *et al.* (2011). The coronal extension of the type $\mathrm{IV_{IP}}$ burst was found to originate from AR10720 and persisted throughout the duration of its interplanetary counterpart. The type II activity, on the other hand, was restricted to the frequency range below 14 MHz. The type III groups accompanying the event were found

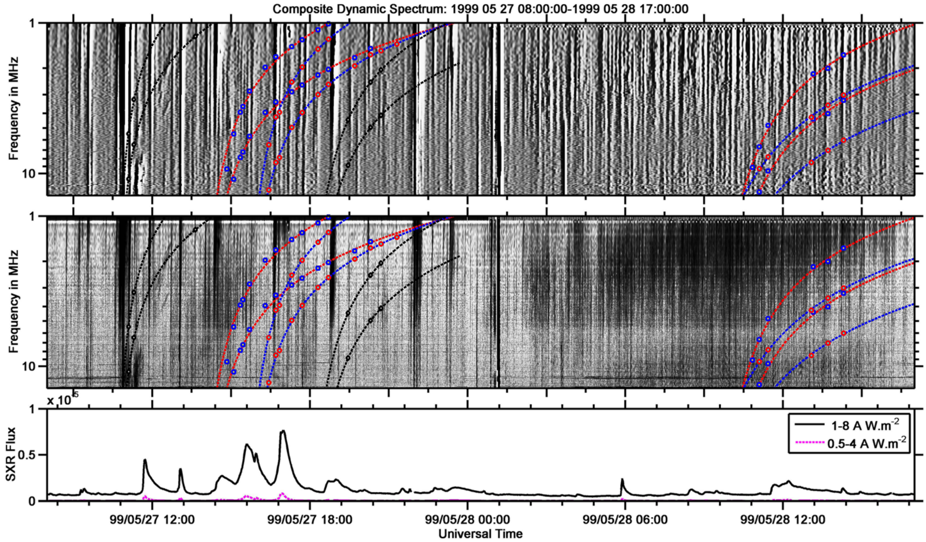

Figure 9 27 – 28 May 1999 event in the period from 27 May 08:00 UT to 28 May 17:00 UT. Top panel: *Wind*/WAVES differential spectrum (inverse grayscale). Middle panel: dynamic (intensity) spectrum. The frequency–time plots derived from the linear fits to the front trajectories of the associated CMEs and an empirical density model (see Section 3.2) for the fundamental and harmonic (thick-dotted curves) plasma emission are overlaid on the spectra. In this example, the CME trajectories are shown with different colors. The squares that mark the positions of the CME fronts are drawn in black on the black trajectories, in red on the blue trajectories, and in blue on the red trajectories (see Section 3.1). Bottom panel: the profiles of GOES SXR 1 – 8 Å (solid black line) and 0.5 – 4 Å (thick-dotted magenta line) flux. The time is in the format date, hours, and minutes.

to overshoot the low-frequency limit of the type $\mathrm{IV_{IP}}$ burst at least after 08:18 UT. Earlier, groups of U-type bursts and type IV fine structures indicated acceleration and partial trapping of electrons behind the CME front.

A detailed study of the radio signatures of this event (Table 1 in Hillaris *et al.*, 2011, which presents a comprehensive outline of its time evolution) points toward possible multiple acceleration mechanisms. These include CME associated shocks in the high corona and the interplanetary space and also shock-independent accelerators at low altitudes associated with the type IV continuum behind the CME.

This event had distinct features of the compact class, *i.e.* it was associated with an intense flare and two fast CMEs, but its long duration characterizes it as extended. Similar to the previous two long-duration events, energetic electrons provided by low corona sources could be associated with the coronal type IV burst.

4. Characteristics of All the Events

4.1. Characteristics of the 45 Compact Events

Of the 48 type $\mathrm{IV_{IP}}$ bursts of our sample 45, classified as compact, were found to conform to the big flare syndrome, which suggests that, statistically, energetic phenomena are more intense in larger flares, regardless of the detailed physics. Nineteen were associated with

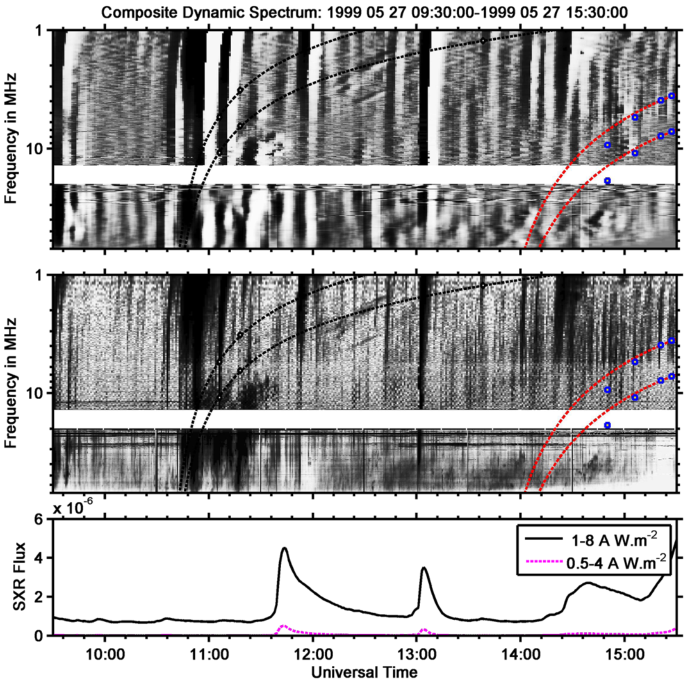

Figure 10 27 – 28 May 1999 event. The panels show the event in the 27 May 09:30 – 15:30 UT period. The dynamic spectra are combined records from the *Wind*/WAVES and the DAM in the 1 – 70 MHz range. This section of the type IV_{IP} starts above 70 MHz and extends to 1 MHz. Top panel: differential spectrum (inverse grayscale). Middle panel: dynamic (intensity) spectrum. The frequency–time plots from the linear fits to the front trajectories of the associated CMEs and the density model presented in Section 3.2, for the fundamental and harmonic (thick-dotted curves) plasma emission are overlaid on the spectra (see Figure 9 for details on these curves). Bottom panel: the profiles of GOES SXR 1 – 8 Å (solid black line) and 0.5 – 4 Å (thick-dotted magenta line) flux.

X-class flares and 21 with M-class, with only five events related to C-class flares. This represents a significant deviation with respect to the general GOES SXR flare distribution studied by Veronig *et al.* (2002). In general, it is expected that ∼66 % of the SXR flares are of class C, with ∼9.5 % of class M, and just ∼0.7 % of class X. The general case is also consistent with the power-law distribution of the peak SXR flux [I], where the probability density, $p(I) \sim I^{-b}$ with $b \approx 2$ (see Aschwanden and Freeland, 2012).

As regards the CME compact-event association, 32 of these events were trailing CMEs with speeds ∼1400 $\mathrm{km\,s^{-1}}$ on average, with only 11 events having CMEs slower than 1000 $\mathrm{km\,s^{-1}}$ (600 – 900 $\mathrm{km\,s^{-1}}$ range). This deviates significantly from the LASCO CME distribution from 1998 to 2011. The comparison of the distributions is presented in Figure 13. The same CMEs were systematically found in the ∼360° tail of the width distribution (see Figure 14). These fast and wide CMEs are expected to transport the type IV emitting energetic electrons confined within their cavities. Bain *et al.* (2014) calculated that the electrons accelerated during the CME initiation or early propagation phase, trapped in the CME magnetic structure, do not need to be replenished for about four hours. This is consistent with the duration of the compact type IV bursts, which is on average about 106 minutes. Furthermore, 43 compact events were characterized by a CME preceding the associated fast CME by some hours along the same path (similar measured position angle in

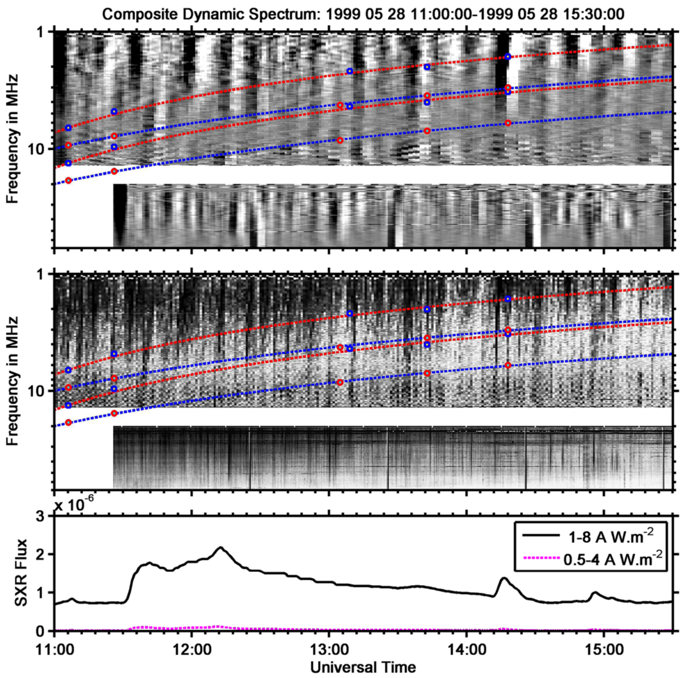

Figure 11 27 – 28 May 1999 event. The panels show the event in the 28 May 11:00 – 15:30 period. The dynamic spectra are combined records from the *Wind*/WAVES and the DAM in the 1 – 70 MHz range. The type $\mathrm{IV_{IP}}$ has a coronal extension above 70 MHz; the most prominent part reaches 1 MHz with some parts extending below this frequency. Top panel: differential spectrum (inverse grayscale). Middle panel: dynamic (intensity) spectrum. The frequency–time plots from the linear fits to the trajectories of the associated CMEs and the density model presented in Section 3.2 for the fundamental and harmonic (thick-dotted curves) plasma emission are overlaid on the spectra (see Figure 9 for details on these curves). Bottom panel: the profiles of GOES SXR 1 – 8 Å (solid black line) and 0.5 – 4 Å (thick-dotted magenta line) flux.

the LASCO CME Catalog), which could have reduced the propagation drag on the trailing CME.

During the interval from 28 October 2003 at 11:30 UT to 29 October at 10:17 UT, no CME was reported in the SOHO/LASCO catalog, but two type $\mathrm{IV_{IP}}$ bursts, in close succession, were recorded by the *Wind*/WAVES. These correspond to entries 28 and 29 in the attached online table and represent two compact events associated with M-class flares. In the column with remarks of the LASCO CME Catalog, the line corresponding to the 28 October 2003 11:30 halo CME and the associated X17.2 flare reports that "all images after 13:00 UT, particularly C3, are severely degraded due to the ongoing proton storm". The non-detection of CMEs associated with the events on 28 and 29 October might therefore be due to this fact.

4.2. Characteristics of the Three Extended Events

The three extended or long-duration type $\mathrm{IV_{IP}}$ events seem to need a resupply of the continuum because they lasted from 960 min to 115 hours (examples in Figures 5 and 9); this requirement holds regardless of the intensity and speed of the first associated flare-CME event. The energetic electron sources in the corona manifest themselves as metric–

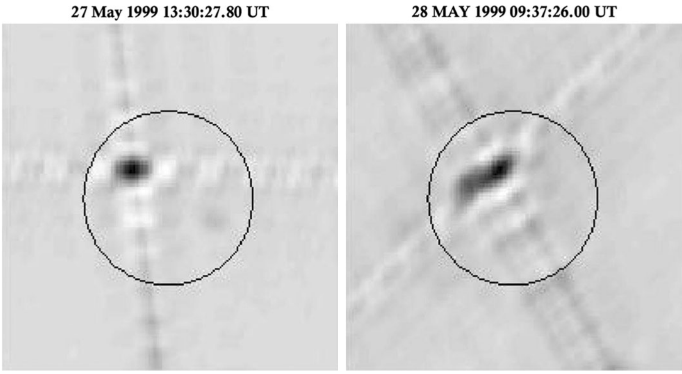

Figure 12 Positions of the coronal type IV bursts in the 27 – 28 May 1999 period, obtained with the *Nançay Radioheliograph* at 164 MHz.

Figure 13 Distribution (%) of CME speeds. (a) LASCO CMEs associated with compact events. (b) All LASCO CMEs in the 1998 – 2012 period for comparison.

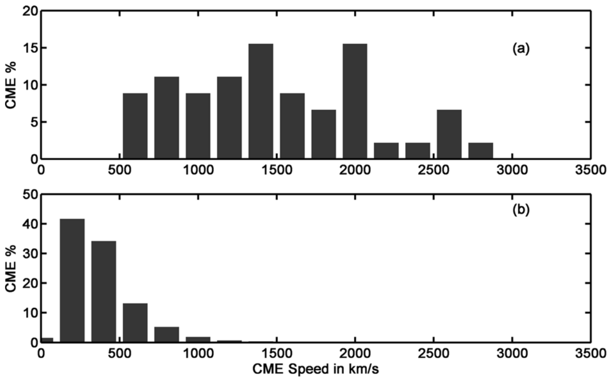

Figure 14 Distribution (%) of CME widths. (a) LASCO CMEs associated with compact events. (b) All LASCO CMEs in the 1998 – 2012 period for comparison.

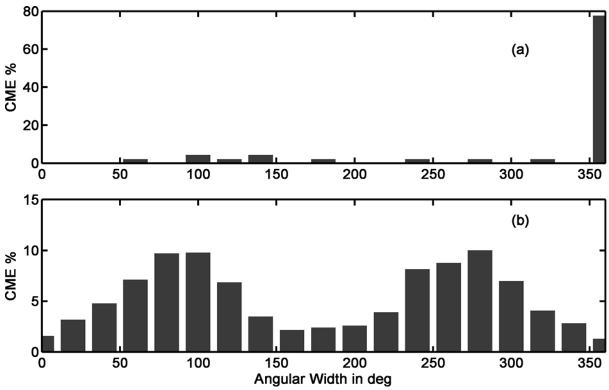

decametric type III and type IV radio bursts. These electron sources need be associated with the lift-off and propagation of CMEs because they deform the solar magnetic field, providing a propagation path for the energetic electrons, and, at the same time, a moving magnetic trap.

In the examples of extended interplanetary type IV bursts discussed in Sections 3.4, 3.5, and 3.6, we see the replenishment process, mentioned above, at work. In all cases we have, in addition to the dynamic spectra, a partial coverage with NRH images. The energetic electron sources in the corona, manifesting themselves as metric and decametric type IV radio bursts, persist in the same position for the duration of each of the interplanetary type IV bursts.

There are other possible sources of energetic electrons, however. First are the type III bursts. They appear to extend in the dynamic spectra far beyond the low-frequency limits of the type IV_{IP} bursts; therefore, a mechanism of electron deposition into the type IV_{IP} is not easily envisaged. The type III-like activity, however, embedded within the type IV continua as part of the type IV fine structure, is linked to the type IV energetic population and the corresponding acceleration process. Another kind of type III-like activity are the micro-type III bursts, which are parts of the IP storms. As they are significantly weaker than the standard type III (six orders of magnitude, see Morioka *et al.*, 2007), they are difficult to detect, especially in their presence, but they cannot be ruled out.

The second possible source is the type IV_{IP} replenishment from the shock-accelerated electrons. The type II bursts mostly appear piston driven by CMEs and preceding the type IV continuum, interplanetary and coronal, which evolves in their wake, possibly within the CME core. This implies a sort of magnetic isolation from energetic populations in the vicinity of the CME bow shock. We note, however, that the possibility of acceleration in the low corona by shocks distinct from those preceding the type IV burst cannot be precluded; the observational confirmation is difficult, however, as these are often buried in other types of radio activity.

5. Discussion and Conclusions

The present study is based on a multi-frequency and multi-instrument study of a sample of 48 interplanetary type IV (type IV_{IP}) bursts identified from the *Wind*/WAVES on line catalog. The dynamic spectra obtained from the *Wind*/WAVES R1 and R2 receivers in the hectometric frequency range are combined with metric and decametric dynamic spectra and supplemented with GOES SXR light curves and LASCO CME data.

In most cases, 45 out of 48, the extension of a metric–decametric moving type IV burst in the hectometric frequency range is found to be associated with a fast and wide CME (see Section 4.1) capable of driving the embedded type IV source into the high corona. This type of bursts has a duration of about 106 minutes on average; these bursts are dubbed compact type IV_{IP} bursts. The reduced aerodynamic drag in the wake of a previous CME, along the same propagation path, appears to increase the probability of the appearance of a type IV_{IP} burst. This preconditioning of the interplanetary space by a previous CME was first proposed, before the discovery of CMEs, by Caroubalos (1964), who stated that a disturbance following a preceding disturbance encounters much more regular conditions than the first. This result points to the effect of CMEs on the structure of the ambient magnetic field and solar wind flow, which in turn controls the propagation behavior of trailing CMEs, as discussed in a number of publications (Vršnak and Žic, 2007; Gopalswamy, 2008; Baker *et al.*, 2013; Vršnak *et al.*, 2014; Liu *et al.*, 2014; Temmer and Nitta, 2015). The basic argument in all cases is that a CME can be subjected to a minimal slowdown in the wake of a preceding CME, as it encounters a preconditioned region of depleted ambient plasma density and almost radial magnetic field lines; within this region, a reduced aerodynamic drag is expected. The efficiency of this effect increases, possibly, if the main CME is quite dense (as discussed by Temmer and Nitta, 2015, based on detailed modelling of a CME propagation). It is also expected that a wide preceding CME would result in a greater drop of the aerodynamic drag compared to a narrow CME along the path of the main CME. Further complications may arise when there is more than one CME preceding the main one as regards CME paths and speeds and the ambiguities in CME mass calculations. Despite these, our results provide qualitative support to the reduced aerodynamic drag postulated by the preconditioning hypothesis.

In addition to the preconditioning of space by a preceding CME that we have discussed in the previous paragraph, the characteristics of these events are consistent with the big flare syndrome since they were mostly associated with medium to large flares and fast CMEs (see Section 4.1). As regards the small number (five of 45) of events associated with smaller flares, we find that either the type IV burst was originating at the solar limb (numbers 37 and 44 in the attached table), or (numbers 35, 42, and 43) the origin of the flare was not known; in both cases the flare association was quite uncertain. There were also intense flares within the period of interest, 1998 – 2012, which did not give type IV_{IP} bursts. This may at least in part be explained by the fact that in the *Wind*/WAVES catalog some events are not listed as type IV bursts. On 20 January 2005, for example, the interplanetary radio signature of the X7.1/2B flare accompanied by a fast ($\approx 900\ \mathrm{km\,s^{-1}}$) halo CME was described as very diffuse. The same holds for the major solar eruption of 7 March 2012 (X5.4 and X1.3 flares associated with two fast ($> 2000\ \mathrm{km\,s^{-1}}$) CMEs, see Patsourakos *et al.*, 2013, 2016); the radio signature is mentioned as strong intermittent multiple tones.

In the three long-duration or extended type IV_{IP} bursts, the energetic electron population, which is the type IV_{IP} source, seems to be replenished from the lower solar corona. This implies the possibility that the type IV_{IP} enclosing magnetic structure is connected to low coronal electron accelerators or coronal reservoirs. The NRH images, when available, indicate that these might be associated with the high-frequency type IV that persists throughout the duration of the extended type IV_{IP} burst.

A steady coronal reservoir of energetic electrons appears to be the metric type IV continuum because most of the type IIIs tend to overshoot the interplanetary type IV. The micro-type III bursts, on the other hand, may trace the electrons' path from the coronal reservoir to the type IV_{IP}. We state at this point that the term coronal reservoir is used to distinguish this region from the heliospheric reservoirs (see Roelof *et al.*, 1992; Sarris and Malandraki, 2003) beyond 1 AU. The fact that the extended type IV_{IP} bursts appear to cumulatively result from relatively small energetic events suggests the presence of some type of trapping structure for the exciter energetic electrons. The type IV_{IP} heliocentric distances, however, are $\sim 25 - 95\ R_{\odot}$, which are much smaller than the distance of 1 AU and beyond of the heliospheric reservoirs. The question of the confinement of the energetic electrons that produce this type of bursts at heliocentric distances on the order of some tens of solar radii remains open.

Acknowledgements This research has been partly cofinanced by the European Union (European Social Fund, ESF) and Greek national funds through the Operational Program Education and Lifelong Learning of the National Strategic Reference Framework (NSRF) – Research Funding Program: Thales. Investing in society knowledge through the European Social Fund. The LASCO CME Catalog is generated and maintained at the CDAW Data Centre by NASA and The Catholic University of America in cooperation with the Naval Research Laboratory. SOHO is a project of international cooperation between ESA and NASA. The *Nançay Radioheliograph* (NRH) is operated by the Observatoire de Paris and funded by the French research agency CNRS/INSU. *The Radio Solar Telescope Network* (RSTN) is a network of solar observatories maintained and operated by the U.S. Air Force Weather Agency. The authors acknowledge the use of the smoothed differentiation filter software by Jianwen Luo. They also thank the anonymous referee for valuable comments and useful suggestions.

Disclosure of Potential Conflicts of Interest The authors declare that they have no conflicts of interest.

Appendix: Comprehensive Catalog of the Type IV_{IP} Burst Records

In Table 1, which is attached as online supplementary material, we provide a summary of the interplanetary type IV bursts recorded by the *Wind*/WAVES R1 and R2 receivers in the 13.825 MHz – 20 kHz frequency range, with their associated CMEs and SXR flares in the 1998 – 2012 period. The coronal extensions of these bursts by the RSTN, DAM, ARTEMIS-IV, *Culgoora*, *Hiraiso*, and IZMIRAN *Radio Spectrographs* are included for comparison.

The headline to each event includes the event number, date of observation, and characterization of the event as compact or extended following the classification introduced in Section 3. Column 1 lists the type of activity; for SXR flares we list the GOES class. The secondary headline, CME preceding main ejection, stands for CMEs preceding the main CME associated with the event by approximately two days along the same path. The path similarity is determined by the comparison of the position angle (PA) and width of the preceding CME to the main. In the extended events, the secondary headline is sometimes absent as they may originate from a number of energetic events (flares and CMEs) and not from a powerful flare or fast CME with the latter propagating in the wake of preceding ejections (see discussion in Section 5). Columns 2 – 3 list start, peak, and end of each type of activity in day, month, hour, and minute (DD MMM HH:MM) format. D indicates that the event extends in time beyond the observation period. The CME start time, in the second column, is the first C2 appearance, while its extrapolated lift-off time appears in the next row as a remark (see below for the description of the remark lines). In the fourth column, we list the SXR flare 1 – 8 Å integrated flux (F_{SXR}^{tot} in $J\,m^{-2}$), and in the same column, the CME speed (V_{CME}) in $km\,s^{-1}$. The location of the flare on the disk and the measured position angle (MPA) of the CMEs with their angular widths in parenthesis are given in the fifth column. The SXR flare location is determined from the position of the associated Hα flare on the disk or the *Solar X-ray Imager* of GOES report if available. In the fifth column, we also report the position of the coronal radio bursts when NRH records are available. In the sixth column we list the frequency range of the radio bursts in MHz; L indicates that the burst extends to lower frequencies, H stands for a high-frequency extension.

Comments and remarks, when necessary, are in separate lines below the description of the activity line. The comments include the reporting stations from which the data of each observation were obtained, together with the classification of the *Wind*/WAVES, the SOHO/LASCO records, and the NOAA active region number of the event. For the flares, the SXR peak and the Hα category when available are reported, while for the CMEs the extrapolated lift-off time is presented. Finally, in the comment lines data gaps are reported (if any).

The reporting observatory or space experiment abbreviations used in Table 1 are as follows:

ART-4	ARTEMIS-IV, Greece
CUL	Culgoora, Australia
SAG	RSTN, Sagamore Hill, Massachusetts, USA
PAL	RSTN, Palehua, Hawaii
HOL	RSTN, Holloman, New Mexico, USA
LEA	RSTN, Learmonth, Australia
SVI	RSTN, San Vito, Italy
RAM	Ramey AFB, Puerto Rico, USA
IZM	IZMIRAN *Radio Spectrograph*
KANZ	*Kanzelhöhe Solar Observatory*

MIT *National Astronomical Observatory of Japan*, Mitaka
HiRAS *Hiraiso Radio Spectrograph*
DAM *Nançay Decameter Array*
NRH *Nançay Radioheliograph*
XFL SXR flare from the GOES *Solar X-ray Imager* (SXI)
Gxx SXR flare from the GOES (for example G08 stands for GOES 08)

All abbreviations, with the exception of NRH, DAM, and ART-4, are adopted from the Space Weather Prediction Center[11] station list.

References

Alissandrakis, C.E., Nindos, A., Patsourakos, S., Kontogeorgos, A., Tsitsipis, P.: 2015, *Astron. Astrophys.* **582**, A52. DOI.
Aschwanden, M.J., Freeland, S.L.: 2012, *Astrophys. J.* **754**, 112. DOI.
Aurass, H., Vršnak, B., Mann, G.: 2002, *Astron. Astrophys.* **384**, 273. DOI.
Aurass, H., Vourlidas, A., Andrews, M.D., Thompson, B.J., Howard, R.H., Mann, G.: 1999, *Astrophys. J.* **511**, 451. DOI.
Bain, H.M., Krucker, S., Saint-Hilaire, P., Raftery, C.L.: 2014, *Astrophys. J.* **782**, 43. DOI.
Baker, D.N., Li, X., Pulkkinen, A., Ngwira, C.M., Mays, M.L., Galvin, A.B., Simunac, K.D.C.: 2013, *Space Weather* **11**, 585. DOI.
Bastian, T.S., Pick, M., Kerdraon, A., Maia, D., Vourlidas, A.: 2001, *Astrophys. J.* **558**, L65. DOI.
Benz, A.O.: 1980, *Astrophys. J.* **240**, 892. DOI.
Boischot, A.: 1957, *C. R. Math.* **244**, 1326.
Boischot, A., Rosolen, C., Aubier, M.G., Daigne, G., Genova, F., Leblanc, Y., *et al.*: 1980, *Icarus* **43**, 399. DOI.
Bougeret, J.-L., Fainberg, J., Stone, R.G.: 1983, *Science* **222**, 506. DOI.
Bougeret, J.-L., Fainberg, J., Stone, R.G.: 1984a, *Astron. Astrophys.* **136**, 255.
Bougeret, J.-L., Fainberg, J., Stone, R.G.: 1984b, *Astron. Astrophys.* **141**, 17.
Bougeret, J.-L., Kaiser, M.L., Kellogg, P.J., Manning, R., Goetz, K., Monson, S.J., *et al.*: 1995, *Space Sci. Rev.* **71**, 231. DOI.
Cane, H.V., Reames, D.V.: 1988, *Astrophys. J.* **325**, 895. DOI.
Caroubalos, C.: 1964, *Ann. Astrophys.* **27**, 333.
Caroubalos, C., Maroulis, D., Patavalis, N., Bougeret, J.-L., Dumas, G., Perche, C., *et al.*: 2001, *Exp. Astron.* **11**, 23. DOI.
Delaboudinière, J.-P., Artzner, G.E., Brunaud, J., Gabriel, A.H., Hochedez, J.F., Millier, F., *et al.*: 1995, *Solar Phys.* **162**, 291. DOI.
Fainberg, J., Stone, R.G.: 1970a, *Solar Phys.* **15**, 222. DOI.
Fainberg, J., Stone, R.G.: 1970b, *Solar Phys.* **15**, 433. DOI.
Fainberg, J., Stone, R.G.: 1971, *Solar Phys.* **17**, 392. DOI.
Gergely, T.E.: 1986, *Solar Phys.* **104**, 175. DOI.
Gopalswamy, N.: 2004, In: Gary, D.E., Keller, C.U. (eds.) *Solar and Space Weather Radiophysics: Current Status and Future Developments*, Kluwer Academic, Dordrecht, 305. DOI.
Gopalswamy, N.: 2008, *J. Atmos. Solar-Terr. Phys.* **70**, 2078. DOI.
Gopalswamy, N.: 2011 In: *Proc. 7th Int. Workshop on Planetary, Solar and Heliospheric Radio Emissions (PRE VII)*, Austrian Acad. Sciences Press, Graz, 325.
Gopalswamy, N., Yashiro, S., Michalek, G., Stenborg, G., Vourlidas, A., Freeland, S., Howard, R.: 2009, *Earth Moon Planets* **104**, 295. DOI.
Gorgutsa, R.V., Gnezdilov, A.A., Markeev, A.K., Sobolev, D.E.: 2001, *Astron. Astrophys. Trans.* **20**, 547. DOI.
Guidice, D.A., Cliver, E.W., Barron, W.R., Kahler, S.: 1981, *Bull. Am. Astron. Soc.* **13**, 553.
Hillaris, A., Malandraki, O., Klein, K.-L., Preka-Papadema, P., Moussas, X., Bouratzis, C., *et al.*: 2011, *Solar Phys.* **273**, 493. DOI.
Kahler, S.W.: 1982, *J. Geophys. Res.* **87**, 3439. DOI.
Kayser, S.E., Bougeret, J.-L., Fainberg, J., Stone, R.G.: 1987, *Solar Phys.* **109**, 107. DOI.

[11] ftp.swpc.noaa.gov/pub/welcome/stations.

Kerdraon, A., Delouis, J.-M.: 1997, In: Trottet, G. (ed.) *Coronal Physics from Radio and Space Observations*, *Lect. Notes Phys.* **483**, Springer, Berlin, 192. ISBN 978-3-540-68693-4. DOI.
Klein, K., Mouradian, Z.: 2002, *Astron. Astrophys.* **381**, 683. DOI.
Klein, K., Krucker, S., Lointier, G., Kerdraon, A.: 2008, *Astron. Astrophys.* **486**, 589. DOI.
Kondo, T., Isobe, T., Igi, S., Watari, S., Tokimura, M.: 1995, *J. Commun. Res. Lab.* **42**, 111.
Kontogeorgos, A., Tsitsipis, P., Caroubalos, C., Moussas, X., Preka-Papadema, P., Hilaris, A., *et al.*: 2006a, *Exp. Astron.* **21**, 41. DOI.
Kontogeorgos, A., Tsitsipis, P., Moussas, X., Preka-Papadema, G., Hillaris, A., *et al.*: 2006b, *Space Sci. Rev.* **122**, 169. DOI.
Kontogeorgos, A., Tsitsipis, P., Caroubalos, C., Moussas, X., Preka-Papadema, P., Hilaris, A., *et al.*: 2008, *Measurement* **41**, 251. DOI.
Lecacheux, A.: 2000 In: *Radio Astronomy at Long Wavelengths*, *Geophys. Monograph. Ser.* **119**, AGU, Washington, 321.
Liu, Y.D., Luhmann, J.G., Kajdič, P., Kilpua, E.K.J., Lugaz, N., Nitta, N.V., *et al.*: 2014, *Nat. Commun.* **5**, 3481. DOI.
Magdalenić, J., Marqué, C., Zhukov, A.N., Vršnak, B., Žic, T.: 2010, *Astrophys. J.* **718**, 266. DOI.
Magdalenić, J., Marqué, C., Zhukov, A.N., Vršnak, B., Veronig, A.: 2012, *Astrophys. J.* **746**, 152. DOI.
Morioka, A., Miyoshi, Y., Masuda, S., Tsuchiya, F., Misawa, H., Matsumoto, H., Hashimoto, K., Oya, H.: 2007, *Astrophys. J.* **657**, 567. DOI.
Nindos, A., Aurass, H., Klein, K.-L., Trottet, G.: 2008, *Solar Phys.* **253**, 3. DOI.
Nindos, A., Alissandrakis, C.E., Hillaris, A., Preka-Papadema, P.: 2011, *Astron. Astrophys.* **531**, A31. DOI.
Patsourakos, S., Vlahos, L., Georgoulis, M., Tziotziou, K., Nindos, A., Podladchikova, O., *et al.*: 2013, In: *11th Hellenic Astron. Conf.*, 10.
Patsourakos, S., Georgoulis, M.K., Vourlidas, A., Nindos, A., Sarris, T., Anagnostopoulos, G., *et al.*: 2016, *Astrophys. J.* **817**, 14. DOI.
Pick, M., Vilmer, N.: 2008, *Astron. Astrophys. Rev.* **16**, 1. DOI.
Pohjolainen, S., Hori, K., Sakurai, T.: 2008, *Solar Phys.* **253**, 291. DOI.
Pohjolainen, S., Khan, J.I., Vilmer, N.: 1999, In: Wilson, A., *et al.* (eds.) *Magnetic Fields and Solar Processes*, *ESA* **SP-448**, 991.
Pohjolainen, S., Maia, D., Pick, M., Vilmer, N., Khan, J.I., Otruba, W., *et al.*: 2001, *Astrophys. J.* **556**, 421. DOI.
Pohjolainen, S., van Driel-Gesztelyi, L., Culhane, J.L., Manoharan, P.K., Elliott, H.A.: 2007, *Solar Phys.* **244**, 167. DOI.
Prestage, N.P., Luckhurst, R.G., Paterson, B.R., Bevins, C.S., Yuile, C.G.: 1994, *Solar Phys.* **150**, 393. DOI.
Reiner, M.J., Kaiser, M.L., Fainberg, J., Bougeret, J.-L.: 2006, *Solar Phys.* **234**, 301. DOI.
Robinson, R.D.: 1978, *Aust. J. Phys.* **31**, 533. DOI.
Robinson, R.D.: 1985, In: McLean, D.J., Labrum, N.R. (eds.) *Solar Radiophysics: Studies of Emission from the Sun at Metre Wavelengths*, Cambridge University Press, Cambridge 385.
Roelof, E.C., Gold, R.E., Simnett, G.M., Tappin, S.J., Armstrong, T.P., Lanzerotti, L.J.: 1992, *Geophys. Res. Lett.* **19**, 1243. DOI.
Sakurai, K.: 1974, *Indian J. Radio Space Phys.* **3**, 289.
Sarris, E.T., Malandraki, O.E.: 2003, *Geophys. Res. Lett.* **30**, 2079. DOI.
Temmer, M., Nitta, N.V.: 2015, *Solar Phys.* **290**, 919. DOI.
Usui, S., Amidror, I.: 1982, *IEEE Trans. Biomed. Eng.* **29**, 686. DOI.
Veronig, A., Temmer, M., Hanslmeier, A., Otruba, W., Messerotti, M.: 2002, *Astron. Astrophys.* **382**, 1070. DOI.
Vršnak, B., Cliver, E.W.: 2008, *Solar Phys.* **253**, 215. DOI.
Vršnak, B., Magdalenić, J., Zlobec, P.: 2004, *Astron. Astrophys.* **413**, 753. DOI.
Vršnak, B., Žic, T.: 2007, *Astron. Astrophys.* **472**, 937. DOI.
Vršnak, B., Temmer, M., Žic, T., Taktakishvili, A., Dumbović, M., Möstl, C., *et al.*: 2014, *Astrophys. J. Suppl.* **213**, 21. DOI.
White, S.M.: 2007, *Asian J. Phys.* **16**, 189.
Yashiro, S., Gopalswamy, N., Michalek, G., St. Cyr, O.C., Plunkett, S.P., Rich, N.B., Howard, R.A.: 2004, *J. Geophys. Res.* **109**(18), 7105. DOI.
Zharkova, V.V., Kosovichev, A.G.: 1999, In: Vial, J.-C., Kaldeich-Schü, B. (eds.) *8th SOHO Workshop: Plasma Dynamics and Diagnostics in the Solar Transition Region and Corona*, *ESA* **SP-446**, 755.

Table 1.: Type IV_{IP} Radio Bursts and Associated Activity

Obs.	Start Universal Time	End	F_{SXR}^{tot} (J m^{-2}) V_{CME} (km s^{-1})	Position PA: Width	Freq. MHz
Compact Event 01: 05 March 2012					
Type IV	05 Mar. 04:15	05 Mar. 07:00			14: 7.0
Type II	05 Mar. 04:00	05 Mar. 12:20			14: 0.4
	Type IV_{IP} and II (F-H), by *Wind*/WAVES				
Type IV	05 Mar. 03:33	05 Mar. 08:33			25L: 500H
	Coronal Type IV by LEA, HiRAS				
Type III	05 Mar. 03:33	05 Mar. 04:48			500: 1.0L
	Two Groups (GG) by *Wind*/WAVES, HiRAS and LEA				
X1.1	05 Mar. 02:30	05 Mar. 04:43	3.70×10^{-1}	N17E52	
	Peak at 04:09, 2B, in AR11429 by G15 and LEA				
CME	05 Mar. 04:00		1531	61° - halo	
	CME Lift-off: 05 Mar. 03:31				
CME(s)Preceding Main Ejection					
CME	05 Mar. 03:12		594	46°(92°)	
CME	04 Mar. 20:48		720	52°(65°)	
CME	04 Mar. 11:00		1306	52° - halo	
Compact Event 02: 04 March 2012					
Type IV	04 Mar. 11:15	04 Mar. 12:15			14: 8.0
Type II	04 Mar. 12:15	04 Mar. 17:00			0.9: 0.3
	Type IV_{IP} and II, by *Wind*/WAVES				
Type IV	04 Mar. 10:00	04 Mar. 12:15		N19E61	550H: 20L
	Coronal Type IV by ART-IV, NRH and SVI				
Type III	04 Mar. 10:58	04 Mar. 11:43			500: 1.0L
	Group (GG) by *Wind*/WAVES, ART-IV, NRH and SVI				
M2.0	04 Mar. 10:29	04 Mar. 12:16	9.20×10^{-2}	N19E61	
	Peak at 10:52, 1N, in AR11429 by G15 and SVI				
CME	04 Mar. 11:00		1306	52° - halo	
	CME Lift-off: 04 Mar. 10:31				
CME(s)Preceding Main Ejection					
CME	04 Mar. 05:00		584	52°(160°)	
	Partiall halo CME				

Table 1.:Type IV_{IP} Radio Bursts and Associated Activity-Continued

Obs.	Start Universal Time	End	F^{tot}_{SXR} (J m^{-2}) V_{CME} (km s^{-1})	Position PA: Width	Freq. MHz
Compact Event 03: 27 January 2012					
Type II	27 Jan. 18:30	28 Jan. 04:45			14: 0.150
Type IV	27 Jan. 18:45	27 Jan. 20:20			14: 10
	Type IV_{IP} and II (F-H, intermittent), by *Wind*/WAVES				
Type II	27 Jan. 18:13	27 Jan. 18:25			25L: 75
Type IV	27 Jan. 18:14	27 Jan. 18:44			25L: 180H
	Coronal Type II and IV by SAG				
Type III	27 Jan. 17:37	27 Jan. 18:31			180H: 1.0L
	Group (GG) by *Wind*/WAVES, and SAG				
X1.7	27 Jan. 17:37	27 Jan. 18:56	3.20×10^{-1}	N27W71	
	Peak at 18:37, 1F, in AR11402 by G15 and HOL				
CME	27 Jan. 18:28		2508	296° - halo	
	CME Lift-off: 27 Jan. 18:14				
CME(s)Preceding Main Ejection					
CME	27 Jan. 03:47		415	230°(92°)	
CME	26 Jan. 04:36		1194	327° - halo	
Compact Event 04: 24 September 2011					
Type IV	24 Sep. 19:45	24 Sep. 21:15			14: 7.0
	Type IV_{IP} by *Wind*/WAVES				
Type IV	24 Sep. 18:30	24 Sep. 20:30			180H: 25L
	Coronal Type IV by LEA				
Type III	24 Sep. 19:09	24 Sep. 21:05			180H: 1.0L
	Four Groups (GG) by *Wind*/WAVES, and LEA				
M3.0	24 Sep. 19:09	24 Sep. 19:41	4.60×10^{-2}	N15E56	
	Peak at 19:21, in AR11302 by G15				
CME	24 Sep. 19:36		972	43° - halo	
	CME Lift-off: 24 Sep. 18:55				
CME(s)Preceding Main Ejection					
CME	24 Sep. 12:48		1915	78° - halo	

Table 1.:Type IV_{IP} Radio Bursts and Associated Activity-Continued

Obs.	Start Universal Time	End	F_{SXR}^{tot} (J m^{-2}) V_{CME} (km s^{-1})	Position PA: Width	Freq. MHz
Compact Event 05: 24 September 2011					
Type IV	24 Sep. 13:00	24 Sep. 14:15			14: 8.0
Type II	24 Sep. 12:50	24 Sep. 22:45			14: 0.3
	Type IV_{IP} and II (Multiple tones), by *Wind*/WAVES				
Type IV	24 Sep. 12:30	24 Sep. 15:00D		N15E56	200: 20L
	Coronal Type IV by ART-IV, DAM and NRH				
Type III	24 Sep. 12:30	24 Sep. 13:26			200H: 1.0L
	by *Wind*/WAVES, ART-IV, DAM and NRH				
M7.1	24 Sep. 12:33	24 Sep. 14:10	2.90×10^{-1}	N15E56	
	Peak at 13:20, 1B, in AR11302 by G15 and HOL				
CME	24 Sep. 12:48		1915	78° - halo	
	CME Lift-off: 24 Sep. 12:33				
CME(s)Preceding Main Ejection					
CME	24 Sep. 09:48		1936	90°(145°)	
Compact Event 06: 22 September 2011					
Type IV	22 Sep. 11:15	22 Sep. 12:30			14: 10
Type II	22 Sep. 11:05	22 Sep. 24:00			14: 0.07
	Type IV_{IP} and II (Multiple tones), by *Wind*/WAVES				
Type IV	22 Sep. 10:38	22 Sep. 14:00		N13E78	180H: 25L
Type II	22 Sep. 10:38	22 Sep. 10:45			100H: 25L
	Coronal Type IV and II by ART-IV, SVI and NRH				
Type III	22 Sep. 10:38	22 Sep. 11:20			180H: 1.0L
	Two Groups (GG) by *Wind*/WAVES, ART-IV, SVI and NRH				
X1.4	22 Sep. 10:29	22 Sep. 1144	4.50×10^{-1}	N13E78	
	Peak at 11:01, 2N, in AR11302 by G15 and SVI				
CME	22 Sep. 10:48		1905	72° - halo	
	CME Lift-off: 22 Sep. 10:28				
CME(s)Preceding Main Ejection					
CME	21 Sep. 22:12		1007	305°(>255°)	
	Uncertain Width, Partial halo.				
CME	21 Sep. 10:12		229	50°(74°)	
CME	21 Sep. 04:36		290	71°(73°)	
	Two Poor Events				

Table 1.:Type IV_{IP} Radio Bursts and Associated Activity-Continued

Obs.	Start Universal Time	End	F_{SXR}^{tot} (J m^{-2}) V_{CME} (km s^{-1})	Position PA: Width	Freq. MHz
Compact Event 07: 14 December 2006					
Type II	14 Dec. 22:30	14 Dec. 23:40			14: 1.5
Type IV	14 Dec. 22:30	14 Dec. 23:45			14: 5.0
		Type IV_{IP} and II, by *Wind*/WAVES			
Type II	14 Dec. 22:06	14 Dec. 22:18			200H: 18L
Type IV	14 Dec. 22:06	14 Dec. 23:30			500H: 18L
		Coronal Type IV(F-H) and II by CUL and HiRAS			
Type III	14 Dec. 22:06	14 Dec. 23:37			300: 1.0L
		Group (GG) by *Wind*/WAVES, CUL and HiRAS			
X1.5	14 Dec. 21:07	14 Dec. 22:26	1.20×10^{-1}	S06W46	
		Peak at 22:15, in AR10930 by G12 and XFL			
CME	14 Dec. 22:30		1042	248° - halo	
		CME Lift-off: 14 Dec. 21:49			
CME(s)Preceding Main Ejection					
CME	13 Dec. 23:48		388	237°(40°)	
CME	13 Dec. 02:54		1774	193° - halo	
CompactEvent 08: 13 December 2006					
Type II	13 Dec. 02:45	13 Dec. 10:40			12: 0.150
Type IV	13 Dec. 03:00	13 Dec. 04:15			14: 7.0
		Type IV_{IP} and II (Fast F-H), by *Wind*/WAVES			
Type II	13 Dec. 02:25	13 Dec. 02:44			300: 20
Type IV	13 Dec. 02:25	13 Dec. 10:00			600H: 20L
		Coronal Type IV and II by CUL, LEA and HiRAS			
Type III	13 Dec. 02:33	13 Dec. 04:07			600H: 1.0L
		Several Groups (GG) by *Wind*/WAVES, CUL, LEA and HiRAS			
X3.4	13 Dec. 02:14	13 Dec. 02:57	5.10×10^{-1}	S06W23	
		Peak at 02:40, 4B, in AR10930 by G12, XFL and LEA			
CME	13 Dec. 02:40		1774	193° - halo	
		CME Lift-off: 13 Dec. 02:19			
CME(s)Preceding Main Ejection					
CME	12 Dec. 21:47		146	207°(75°)	
CME	12 Dec. 20:28		474	198°(50°)	

Table 1.:Type IV_{IP} Radio Bursts and Associated Activity-Continued

Obs.	Start Universal Time	End	F_{SXR}^{tot} (J m^{-2}) V_{CME} (km s^{-1})	Position PA: Width	Freq. MHz
Compact Event 09: 13 September 2005					
Type IV	13 Sep. 20:05	13 Sep. 21:00			14: 3.0
Type II	13 Sep. 20:20	15 Sep. 06:00			1.1: 0.035
	Type IV_{IP} and II, by *Wind*/WAVES				
Type IV	13 Sep. 19:44	13 Sep. 22:00			180H: 25L
Type II	13 Sep. 19:45	13 Sep. 20:20			80: 25L
	Coronal Type IV and II by PAL and SAG				
Type III	13 Sep. 19:40	13 Sep. 20:09			180H: 1.0L
	Two Groups (GG) by *Wind*/WAVES, PAL and SAG				
X1.5	13 Sep. 19:19	13 Sep. 20:57	5.50×10^{-1}	S09E10	
	Peak at 19:27 (Second Peak at 20:05), 2B, in AR10808 by G12 and HOL				
CME	13 Sep. 20:00		1866	149° - halo	
	CME Lift-off: 13 Sep. 19:35				
CME(s)Preceding Main Ejection					
CME	12 Sep. 09:12		511	135°(22°)	
CME	11 Sep. 13:01		1922	125° - halo	
Compact Event 10: 09 September 2005					
Type IV	09 Sep. 20:15	09 Sep. 21:10			14: 5.0
Type II	09 Sep. 19:45	09 Sep. 22:00			10: 0.05
	Type II (diffuse) and IV_{IP} by *Wind*/WAVES				
Type IV	09 Sep. 19:34	09 Sep. 21:23			180H: 25L
Type II	09 Sep. 19:34	09 Sep. 19:49			180: 25L
	Coronal Type IV and II by PAL and HOL				
Type III	09 Sep. 19:30	09 Sep. 20:17			180H: 1.0L
	Group (GG) by *Wind*/WAVES, PAL and HOL				
X6.2	09 Sep. 19:13	09 Sep. 20:36	1.70	S12E58	
	Peak at 20:04, 2B, in AR10808 by G12, XFL and HOL				
CME	09 Sep. 19:48		2257	115° - halo	
	CME Lift-off: 09 Sep. 19:30				
CME(s)Preceding Main Ejection					
CME	07 Sep. 05:48		195	85°(74°)	

Table 1.:Type IV_{IP} Radio Bursts and Associated Activity-Continued

Obs.	Start Universal Time	End	F_{SXR}^{tot} (J m^{-2}) V_{CME} (km s^{-1})	Position PA: Width	Freq. MHz
Compact Event 11: 22 August 2005					
Type IV	22 Aug. 01:45	22 Aug. 03:15			14: 10
Type II	22 Aug. 01:30	22 Aug. 03:35			8: 0.550
	Type II (Strong F, weak H) and Type IV_{IP} Weak, by *Wind*/WAVES				
Type IV	22 Aug. 00:59	22 Aug. 04:00D			500H: 20L
Type II	22 Aug. 01:00	22 Aug. 01:45			200: 20L
	Coronal Type II and IV, by CUL and HiRAS				
Type III	22 Aug. 01:01	22 Aug. 01:22			100: 1.0L
	Group (GG) by *Wind*/WAVES, CUL and HiRAS				
M2.6	22 Aug. 00:44	22 Aug. 02:18	9.60×10^{-2}	S11W54	
	Peak at 01:33, 1F, in AR10798 by G12, XFL and LEA				
CME	22 Aug. 01:32		1194	220° - halo	
	CME Lift-off: 22 Aug. 0:52				
CME(s)Preceding Main Ejection					
CME	21 Aug. 12:06		287	255°(61°)	
	C2 Only				
Compact Event 12: 11 May 2005					
Type IV	11 May 20:05	11 May 20:20			14: 8.0
Type II	11 May 20:05	11 May 20:35			14: 2.5
	Type II (F-H) and IV_{IP}, by *Wind*/WAVES				
Type II	11 May 19:29	11 May 21:00			180H: 4L
Type IV	11 May 19:40	11 May 21:00D			180H: 25L
	Coronal TypeII and IV by PAL				
Type III	11 May 19:30	11 May 19:53			180H: 1.0L
	Two Groups (GG) by *Wind*/WAVES and PAL				
M1.1	11 May 19:22	11 May 19:55	1.60×10^{-2}	S10W47	
	Peak at 19:38, 1F, in AR10758 by G12, HOL and XFL				
CME	11 May 20:13		550	232° - halo	
	CME Lift-off: 11 May 18:36				
CME(s)Preceding Main Ejection					
CME	11 May 07:32		305	238°(95°)	
CME	10 May 16:06		609	275° - halo	

Table 1.:Type IV_{IP} Radio Bursts and Associated Activity-Continued

Obs.	Start Universal Time	End	F_{SXR}^{tot} (J m^{-2}) V_{CME} (km s^{-1})	Position PA: Width	Freq. MHz
Compact Event 13: 19 January 2005					
Type IV	19 Jan. 08:45	19 Jan. 09:55			14: 4.50
Type II	19 Jan. 09:20	19 Jan. 24:00			5.3: 0.040
	Type II (Complex, intermittent) and IV_{IP}, by *Wind*/WAVES				
Type II	19 Jan. 08:12	19 Jan. 08:20			300: 20L
Type IV	19 Jan. 08:05	19 Jan. 10:50D		N15W51	600: 20L
	Coronal Type IV and II by ART-IV and NRH				
Type III	19 Jan. 08:14	19 Jan. 08:45			400: 1.0L
	Two Groups by *Wind*/WAVES, ART-4 and NRH				
M6.7	19 Jan. 06:58	19 Jan. 07:55	7.7×10^{-2}	N15W51	
	Peak at 07:31, in AR10720 by G12 and XFL				
X1.3	19 Jan. 08:03	19 Jan. 08:40	2.20×10^{-1}	N15W51	
	Peak at 08:22, 2N, in AR10720 by G12, LEA and XFL				
CME	19 Jan. 08:29		2020	320° - halo	
	CME Lift-off: 19 Jan. 08:02				
CME(s)Preceding Main Ejection					
CME	18 Jan. 17:14		287	305°(43°)	
CME	17 Jan. 09:30		2094	334° - halo	
CME	17 Jan. 09:54		2547	309° - halo	
Extended Event 14: 17 January 2005					
Type IV	17 Jan. 10:00	18 Jan. 02:00			14: 4.0
Type II	17 Jan. 09:25	18 Jan. 16:00			14: 0.030
	Complex, Multi-component Type II and Longest Duration IV_{IP}, by *Wind*/WAVES				
Type IV	17 Jan. 08:40	17 Jan. 15:24D		N15W25	630: 20L
	Coronal Type IV and II by ART-IV and NRH				
Type IV	17 Jan. 17:17	18 Jan. 03:00D			630H: 20L
	Coronal Type IV and II by CUL, PAL and LEA				
Type III	17 Jan. 09:07	17 Jan. 09:59			630: 1.0L
	Two Groups (GG) by *Wind*/WAVES, ART-4 and NRH				
X3.8	17 Jan. 06:59	17 Jan. 10:07	8.40×10^{-01}	N15W25	
	Peak at 09:52, 3B, in AR10720 by G12, XFL and KANZ				
CME	17 Jan. 09:54		2547	309° - halo	
	CME Lift-off:17 Jan. 09:38				
CME(s)Preceding Main Ejection					
CME	17 Jan. 09:30		2094	334° - halo	

Table 1.:Type IV_{IP} Radio Bursts and Associated Activity-Continued

Obs.	Start Universal Time	End	F^{tot}_{SXR} (J m^{-2}) V_{CME} (km s^{-1})	Position PA: Width	Freq. MHz
Compact Event 15: 15 January 2005					
Type IV	15 Jan. 23:30	16 Jan. 02:00			14: 7.0
Type II	15 Jan. 23:00	16 Jan. 24:00			3: 0.040
Type II (Fast Multi-component) and IV_{IP}, by *Wind*/WAVES					
Type IV	15 Jan. 22:30	16 Jan. 03:00D			500H: 30L
Type II	15 Jan. 22:36	15 Jan. 23:00			200: 30L
Coronal Type IV and II by CUL					
Type III	15 Jan. 22:33	15 Jan. 23:08			180: 1.0L
Group (GG) by *Wind*/WAVES, and CUL					
X2.6	15 Jan. 22:25	0115 23:31	6.30×10^{-01}	N15W05	
Peak at 23:02, in AR10720 by G12 and XFL					
CME	15 Jan. 23:07		2861	323° - halo	
CME Lift-off:15 Jan. 22:36					
CME(s)Preceding Main Ejection					
CME	15 Jan. 06:30		2049	359° - halo	
Compact Event 16: 15 January 2005					
Type IV	15 Jan. 07:00	15 Jan. 08:30			14: 7.0
Type II	15 Jan. 06:15	15 Jan. 09:30			14: 0.250
Type II (Chaotic) and IV_{IP}, by *Wind*/WAVES					
Type IV	15 Jan. 06:00	15 Jan. 10:00D		N11E06°	630: 20L
Coronal Type IV by ART-IV and NRH					
Type III	15 Jan. 06:06	15 Jan. 06:40			630: 1.0L
Group by *Wind*/WAVES, ART-4 and NRH					
M8.6	15 Jan. 05:54	15 Jan. 07:17	2.90×10^{-1}	N11E06°	
Peak at 06:38, SF, in AR10720 by G12, XFL and LEA					
CME	15 Jan. 06:30		2049	359° - halo	
CME Lift-off:15 Jan. 05:57					
CME(s)Preceding Main Ejection					
CME	14 Jan. 17:06		358	238° - halo	
Poor Event, Only C2					
CME	13 Jan. 23:54		335	058°>250°	
Uncertain Width, Partial halo					

Table 1.:Type IV_{IP} Radio Bursts and Associated Activity-Continued

Obs.	Start Universal Time	End	F_{SXR}^{tot} (J m^{-2}) V_{CME} (km s^{-1})	Position PA: Width	Freq. MHz
Compact Event 17: 09 November 2004					
Type IV	09 Nov. 17:50	09 Nov. 19:50			14: 7.0
Type II	09 Nov. 17:35	09 Nov. 18:10			14: 5.0
Type II (Intermittent Tone) and IV_{IP}, by *Wind*/WAVES					
Type II	09 Nov. 17:24	09 Nov. 17:30			40: 25L
Type IV	09 Nov. 17:06	09 Nov. 20:30D			180H: 25L
Coronal Type IV and II by SAG					
Type III	09 Nov. 17:00	09 Nov. 17:30			180H: 1.0L
Group by *Wind*/WAVES, and SAG					
M8.9	09 Nov. 16:59	09 Nov. 17:32	9.40×10^{-2}	N08W51	
Peak at 17:19, 2N, in AR10696 by G12, XFL and HOL					
CME	09 Nov. 17:26		2000	299° - halo	
CME Lift-off: 09 Nov. 16:57					
CME(s)Preceding Main Ejection					
CME	09 Nov. 01:28		282	295°(26°)	
CME	08 Nov. 11:54		557	310°(27°)	
CME	08 Nov. 14:54		605	307°(23°)	
CME	08 Nov. 03:54		462	148° - halo	
Compact Event 18: 07 November 2004					
Type IV	07 Nov. 17:10	07 Nov. 18:15			14: 10
Type II	07 Nov. 16:25	08 Nov. 20:00			14: 0.060
Type II (Chaotic with multiple tones) and IV_{IP}, by *Wind*/WAVES					
Type II	07 Nov. 15:59	07 Nov. 16:16			180H: 25L
Type IV	07 Nov. 16:00	07 Nov. 19:00D			180H: 25L
Coronal Type IV and II by SAG					
Type III	07 Nov. 15:59	07 Nov. 16:57			180H: 1.0L
Group (GG) by *Wind*/WAVES, and SAG					
X2.0	07 Nov. 15:42	07 Nov. 16:15	2.00×10^{-1}	N09W17	
Peak at 16:06, in AR10696 by G12 and XFL					
CME	07 Nov. 16:54		1759	00° - halo	
CME Lift-off: 07 Nov. 16:16					
CME(s)Preceding Main Ejection					
CME	07 Nov. 14:30		226	298°(100°)	
CME	06 Nov. 02:06		1111	21°(>214°)	
Poor Event with Uncertain Width, Partial halo					
CME	06 Nov. 01:32		818	23° - halo	

Table 1.:Type IV_{IP} Radio Bursts and Associated Activity-Continued

Obs.	Start Universal Time	End	F^{tot}_{SXR} (J m^{-2}) V_{CME} (km s^{-1})	Position PA: Width	Freq. MHz
Compact Event 19: 06 November 2004					
Type IV	06 Nov. 01:20	06 Nov. 02:30			14: 10
Type II	06 Nov. 01:50	06 Nov. 02:45			6: 0.70
	Type II and IV_{IP}, by *Wind*/WAVES				
Type IV	06 Nov. 00:33	06 Nov. 02:45			1000: 18L
Type II	06 Nov. 00:44	06 Nov. 00:58			80: 25
	Coronal Type IV and II by LEA and CUL				
Type III	06 Nov. 00:44	06 Nov. 00:58			1000: 1.0L
Type III	06 Nov. 01:40	06 Nov. 01:43			1000: 1.0L
	Two Groups by *Wind*/WAVES and CUL				
M9.3	06 Nov. 00:11	06 Nov. 00:42	6.50×10^{-2}	N10E08	
	Peak at 00:34 , 2N, in 10696 by G12, XFL and LEA				
M5.9	06 Nov. 00:44	06 Nov. 01:10	8.50×10^{-2}	N10E05	
	Peak at 00:57 , 1N, in 10696 by G12 and CUL				
M3.6	06 Nov. 01:40	06 Nov. 02:08	5.50×10^{-2}	N07E00	
	Peak at 01:57, 1N, in AR10696 by G12 and CUL				
CME	06 Nov. 01:32		818	23° - halo	
	CME Lift-off: 06 Nov. 00:38				
CME(s)Preceding Main Ejection					
CME	06 Nov. 02:06		1111	21°(>214°)	
	Poor Event with Uncertain Width, Partial halo				
CME	06 Nov. 23:30		1055	31°(>293°)	
	Uncertain Width; Partial halo				
Compact Event 20: 29 July 2004					
Type IV	29 July 12:40	29 July 14:30			14: 3.0
Type II	29 July 13:20	29 July 20:30			1.0: 0.05
	Type II (Continuous tone with structure) and IV_{IP}, by *Wind*/WAVES				
Type IV	29 July 11:30	29 July 13:30		S00W90	180H: 25L
	Coronal Type IV by SVI				
Type III	29 July 10:57	29 July 12:26			180H: 1.0L
	Several Grours (GG and G) by *Wind*/WAVES, and SVI				
C2.1	29 July 11:42	29 July 14:02	1.20×10^{-2}		
	Peak at 13:04, in AR10652 by G12				
CME	29 July 12:06		1180	245° - halo	
	CME Lift-off: 29 July 11:51				
CME(s)Preceding Main Ejection					
CME	29 July 09:30		275	241°(48°)	
CME	28 July 03:30		754	284°(>201°)	
	Uncertain Width, Partial halo				

Table 1.:Type IV_{IP} Radio Bursts and Associated Activity-Continued

Obs.	Start Universal Time	End	F_{SXR}^{tot} (J m^{-2}) V_{CME} (km s^{-1})	Position PA: Width	Freq. MHz
Compact Event 21: 25 July 2004					
Type IV	25 July 15:10	25 July 20:30			14: 2.0
Type II	25 July 15:00	26 July 22:25			1.0: 0.028
	Type II (Complex with many bands) and IV_{IP}, by *Wind*/WAVES				
Type IV	25 July 14:15	25 July 17:31		N04W30	180H: 25L
	Coronal Type IV by SVI and NRH				
Type III	24 July 13:18	24 July 15:10			180H: 1.0L
	Type III Groups by *Wind*/WAVES, and SVI				
C2.1	24 July 13:18	24 July 13:32	1.50×10^{-3}	N04W29	
	Peak at 13:25, in AR10652 by G12 and XFL				
M2.2	24 July 13:37	24 July 13:55	1.30×10^{-2}	N04W30	
	Peak at 13:49, in AR10652 by G12 and XFL				
M1.1	25 July 14:19	25 July 16:43	6.50×10^{-2}	N08W33	
	Peak at 15:14, 1F, in AR10652 by G12 and HOL				
CME	25 July 14:54		1333	204° - halo	
	CME Lift-off: 25 July 14:32				
CME(s)Preceding Main Ejection					
CME	25 July 14:30		450	229°(45°)	
CME	25 July 13:32		556	242°(16°)	
CME	25 July 06:54		299	296°(31°)	
CME	24 July 23:54		555	215°(78°)	
Compact Event 22: 23 July 2004					
Type IV	23 July 19:30	23 July 20:30			14: 7.0
Type II	23 July 19:00	23 July 19:35			1: 2.5
	Type II and IV_{IP}, by *Wind*/WAVES				
Type IV	23 July 18:30	23 July 21:30			180H: 25L
	Coronal Type IV by PAL				
Type III	23 July 17:30	23 July 18:30			180H: 1.0L
	Type III Group (GG) by *Wind*/WAVES, and PAL				
M2.2	23 July 17:07	23 July 17:35	1.50×10^{-2}	N04W08	
	Peak at 17:28, in AR10652 by G12 and XFL				
C4.1	23 July 18:02	23 July 18:11	1.70×10^{-3}	N05W05	
	Peak at 18:07, in AR10652 by G12 and XFL				
M1.7	23 July 21:15	23 July 21:30	9.00×10^{-3}	N05W07	
	Peak at 21:23, in AR10652 by G12 and XFL				
CME	23 July 19:32		874	187°(100°)	
	CME Lift-off: 23 July 18:47				

Table 1.:Type IV_{IP} Radio Bursts and Associated Activity-Continued

Obs.	Start	End	F_{SXR}^{tot}	Position	Freq.
	Universal Time		(J m^{-2})	PA: Width	MHz
			V_{CME}		
			(km s^{-1})		
CME(s)Preceding Main Ejection					
CME	23 July 16:06		824	278° - halo	
CME	23 July 17:54		569	256°(142°)	
CME	23 July 07:32		459	218°(138°)	
		Two Partial haloes			
Compact Event 23: 04 November 2003					
Type IV	04 Nov. 20:20	04 Nov. 21:00			14: 10
Type II	04 Nov. 20:00	04 Nov. 24:00			10: 0.20
		Type II and IV_{IP}, by *Wind*/WAVES			
Type IV	04 Nov. 19:35	04 Nov. 21:00			300H: 25L
		Coronal Type IV by HOL and CUL (after 20:00)			
Type III	04 Nov. 19:35	04 Nov. 20:38			180H: 1.0L
		Type III Groups by *Wind*/WAVES, and HOL			
X17.4	04 Nov. 19:29	04 Nov. 20:06	2.30	S19W83	
		Peak at 19:53, 3B, in AR10486 by G12 and HOL			
CME	04 Nov. 19:54		2657	260° - halo	
		CME Lift-off: 04 Nov. 19:38, 3 Points			
CME(s)Preceding Main Ejection					
CME	04 Nov. 19:32		327	187°(52°)	
CME	04 Nov. 12:54		605	263°(72°)	
CME	04 Nov. 12:06		1208	84° - halo	
Compact Event 24: 03 November 2003					
Type IV	03 Nov. 10:15	03 Nov. 11:15			14: 6.0
Type II	03 Nov. 10:00	03 Nov. 12:30			6: 0.40
		Type II (Complex F-H) and IV_{IP} (with drifting features), by *Wind*/WAVES			
Type IV	03 Nov. 09:50	03 Nov. 11:40		N08W77	500: 20L
Type II	03 Nov. 09:51	03 Nov. 10:12			200: 20L
		Coronal Type IV and II by ART-IV and NRH			
Type III	03 Nov. 09:49	03 Nov. 10:05			500H: 1.0L
		Groups (GG) by *Wind*/WAVES, ART-IV and NRH			
X3.9	03 Nov. 09:43	03 Nov. 10:19	5.60×10^{-1}	N08W77	
		Peak at 09:55, 2F, in AR10488 by G12 and LEA			
CME	03 Nov. 10:06		1420	301°(103°)	
		CME Lift-off:03 Nov. 09:45			
CME(s)Preceding Main Ejection					
CME	03 Nov. 01:59		827	324°(65°)	

Table 1.:Type IV_{IP} Radio Bursts and Associated Activity-Continued

Obs.	Start Universal Time	End	F^{tot}_{SXR} (J m^{-2}) V_{CME} (km s^{-1})	Position PA: Width	Freq. MHz
Compact Event 25: 03 November 2003					
Type IV	03 Nov. 02:10	03 Nov. 03:05			14: 9.0
Type II	03 Nov. 01:15	03 Nov. 01:25			3.0: 1.5
TypeII (Multiple brief tones) and IV_{IP}, by *Wind*/WAVES					
Type IV	03 Nov. 01:31	03 Nov. 04:00			500H: 18L
Type II	03 Nov. 01:24	03 Nov. 01:30			200: 18L
Coronal Type IV and II by CUL and LEA					
Type III	03 Nov. 00:58	03 Nov. 01:34			250: 1.0L
Group (GG) by *Wind*/WAVES and CUL					
X2.7	03 Nov. 01:09	03 Nov. 01:45	3.60×10^{-1}	N10W83	
Peak at 01:30, 2B, in AR10488 by G12 and LEA					
CME	03 Nov. 01:59		827	324°(65°)	
CME Lift-off:03 Nov. 00:52					
CME(s)Preceding Main Ejection					
CME	01 Nov. 21:30		413	320°(>143°)	
Uncertain Width, Partial halo					
Compact Event 26: 02 November 2003					
Type IV	02 Nov. 17:55	02 Nov. 18:50			14: 8.0
Type II	02 Nov. 17:30	03 Nov. 01:00			12: 0.25
Type II (Chaotic and intense) and IV_{IP}, by *Wind*/WAVES					
Type IV	02 Nov. 17:14	02 Nov. 18:24			80: 25L
Type II	02 Nov. 17:14	02 Nov. 17:37			180: 25L
Coronal Type IV and II by HOL					
Type III	02 Nov. 17:14	02 Nov. 17:48			180: 1.0L
Group (GG) by *Wind*/WAVES and HOL					
X8.3	02 Nov. 17:03	02 Nov. 17:39	9.10×10^{-1}	S14W56	
Peak at 17:25, 2B, in AR10486 by G12 and HOL					
CME	02 Nov. 17:30		2598	265° - halo	
CME Lift-off:02 Nov. 17:16					
CME(s)Preceding Main Ejection					
CME	02 Nov. 11:30		826	226°(33°)	
CME	02 Nov. 09:30		2036	195° - halo	

Table 1.:Type IV_{IP} Radio Bursts and Associated Activity-Continued

Obs.	Start Universal Time	End	F_{SXR}^{tot} (J m^{-2}) V_{CME} (km s^{-1})	Position PA: Width	Freq. MHz
Compact Event 27: 29 October 2003					
Type IV	29 Oct. 21:15	29 Oct. 22:30			14: 5.0
Type II	29 Oct. 20:55	29 Oct. 24:00			11: 0.50
	Type II (Difficult to observe) and IV_{IP}, by *Wind*/WAVES				
Type IV	29 Oct. 20:39	29 Oct. 21:00D			500H: 20L
Type II	29 Oct. 20:42	29 Oct. 20:55			18: 430
	Coronal Type IV and II by CUL				
Type III	29 Oct. 20:49	29 Oct. 21:00			500H: 1.0L
	Group (GG) by *Wind*/WAVES and CUL				
X10.0	29 Oct. 20:37	29 Oct. 21:01	8.70×10^{-1}	S15W02	
	Peak at 20:49, 2B, in AR10486 by G12 and HOL				
CME	29 Oct. 20:54		2029	190° - halo	
	CME Lift-off:29 Oct. 20:36				
CME(s)Preceding Main Ejection					
CME	29 Oct. 10:17		922	182°(114°)	
	Very Poor Event, C2 Only.				
Compact Event 28: 29 October 2003					
Type IV	29 Oct. 06:00	29 Oct. 11:00			14: 9.0
	Type IV_{IP}, by *Wind*/WAVES				
Type IV	29 Oct. 05:35	29 Oct. 13:00D		S20W08	200: 20L
	Coronal Type IV and II by ART-IV, SVI, HOL and NRH (after 10:00)				
Type III	29 Oct. 04:27	29 Oct. 10:00			180H: 1.0L
	Groups (GG) by *Wind*/WAVES, ART-4 and SVI				
M3.5	29 Oct. 04:08	29 Oct. 05:54	1.20×10^{-1}	S17E06	
	Peak at 05:11, SN, in AR10486 by G12 and LEA				
CME	29 Oct. 10:17		922	200°(114°)	
	CME Lift-off:29 Oct. 09:00, Very Poor Event, C3 Only				
NO LASCO CMEs recorded from 28 October 11:30 to 29 October 10:17 UT.					
Compact Event 29: 29 October 2003					
Type IV	29 Oct. 01:30	29 Oct. 04:00			14: 7.0
	Type IV_{IP}, by *Wind*/WAVES				
Type IV	29 Oct. 00:37	29 Oct. 03:55D			180H: 25L
	Coronal Type IV and II by LEA				
Type III	29 Oct. 00:21	29 Oct. 01:29			180H: 1.0L
	by *Wind*/WAVES and LEA				
M1.1	29 Oct. 00:26	29 Oct. 02:08	5.20×10^{-02}	S18E08	
	Peak at 01:51, 1F, in AR10486 by G12 and LEA				
NO LASCO CMEs recorded from 28 October 11:30 to 29 October 10:17 UT.					

Table 1.:Type IV_{IP} Radio Bursts and Associated Activity-Continued

Obs.	Start Universal Time	End	F^{tot}_{SXR} (J m^{-2}) V_{CME} (km s^{-1})	Position PA: Width	Freq. MHz
Compact Event 30: 28 October 2003					
Type IV	28 Oct. 11:30	28 Oct. 15:00			14: 5.0
Type II	28 Oct. 11:10	29 Oct. 24:00			14: 0.04
Strongest type II and IV_{IP} observed by *Wind*/WAVES					
Type IV	28 Oct. 10:38	28 Oct. 14:00D		S16E08	550: 20L
Type II	28 Oct. 11:05	28 Oct. 11:17			550: 20L
Coronal Type IV and II by ART-IV and NRH (after 10:00)					
Type III	28 Oct. 10:58		28 Oct. 11:22		550: 1.0L
Group (GG) by *Wind*/WAVES, and ART-IV					
X17.2	28 Oct. 09:51	1028 11:24	1.80	S16E08	
Peak at 11:10, 4B, in AR10486 by G12 and SVI					
CME	28 Oct. 11:30		2459	15° - halo	
CME Lift-off: 28 Oct. 11:01					
CME(s)Preceding Main Ejection					
CME	28 Oct. 09:30		853	86°(22°)	
CME	27 Oct. 20:30		990	322°(43°)	
CME	27 Oct. 13:32		1005	326°(45°)	
Compact Event 31: 28 May 2003					
Type IV	28 May 01:00	28 May 03:00			14: 10
Type IV_{IP}, by *Wind*/WAVES					
Type IV	28 May 00:23	28 May 02:41			500H: 40
Coronal Type IV by CUL					
Type III	28 May 00:23	28 May 01:14			500H: 1.0L
Two Groups (GG) by *Wind*/WAVES and CUL					
X3.6	28 May 00:17	28 May 00:39	2.80×10^{-1}	S08W22	
Peak at 00:27, 1B, in AR10365 by G12 and MIT					
CME	28 May 00:50		1366	292° - halo	
CME Lift-off: 28 May 00:13					
CME(s)Preceding Main Ejection					
CME	27 May 23:50		964	67° - halo	
CME	27 May 22:06		1122	225°(123°)	
CME Lift-off: 25 Apr. 05:04, Partial halo					

Table 1.:Type IV_{IP} Radio Bursts and Associated Activity-Continued

Obs.	Start Universal Time	End	F_{SXR}^{tot} (J m^{-2}) V_{CME} (km s^{-1})	Position PA: Width	Freq. MHz
Compact Event 32: 25 April 2003					
Type IV	25 Apr. 05:55	25 Apr. 06:10			14: 9.0
		Type IV_{IP}, by *Wind*/WAVES			
Type IV	25 Apr. 05:31	25 Apr. 05:46			124: 25L
Type II	25 Apr. 05:41	25 Apr. 05:55			180: 25L
	Coronal Type IV and II (F-M) by CUL and LEA				
Type III	25 Apr. 05:24	25 Apr. 05:56			360: 1.0L
	Three Goups (GG) by *Wind*/WAVES, CUL and LEA				
M1.2	25 Apr. 05:23	25 Apr. 05:58	1.80×10^{-2}	N14E79	
	Peak at 05:40, SF, in AR10346 by G10 and LEA				
CME	25 Apr. 05:50		806	54°(235°)	
	CME Lift-off: 25 Apr. 05:04, Partial halo				
CME(s)Preceding Main Ejection					
CME	24 Apr. 02:50	459	51°(138°)		
		Poor Event.			
CME	24 Apr. 22:26		347	59°(47°)	
Compact Event 33: 16 August 2002					
Type IV	16 Aug. 12:20	16 Aug. 16:30			14: 4.0
Type II	16 Aug. 12:20	17 Aug. 21:00			14: 0.060
	Type IV_{IP} and II (Multiple bands), by *Wind*/WAVES				
Type IV	16 Aug. 12:05	16 Aug. 17:56D		S14E20	180H: 25L
	Coronal Type IV by SVI and NRH				
Type III	16 Aug. 11:32	16 Aug. 13:00			180H: 1.0L
	Several Groups (G–GG) by *Wind*/WAVES, SVI and NRH				
M5.2	16 Aug. 11:32	16 Aug. 13:07	1.60×10^{-1}	S14E20	
	Peak at 12:32, 2N, in AR10069 by G08 and SVI				
CME	16 Aug. 12:30		1585	121° - halo	
	CME Lift-off: 16 Aug. 12:01				
CME(s)Preceding Main Ejection					
CME	14 Aug. 10:54		809	142°(52°)	
CME	14 Aug. 16:54		1049	100°(16°)	
		3 points only.			
Extended Event 34: 18-23 May 2002					
Type IV	18 May 09:00	23 May 04:00			9: 0.400
	Possible moving Type IV_{IP}, by *Wind*/WAVES. Very intense				
CME	18 May 08:06		841	90°(6°)	
	CME Lift-off: 18 May 07:00, Only 2 points				
CME	18 May 09:26		707	226°(78°)	
	CME Lift-off: 18 May 08:27				

Table 1.:Type IV_{IP} Radio Bursts and Associated Activity-Continued

Obs.	Start Universal Time	End	F_{SXR}^{tot} (J m^{-2}) V_{CME} (km s^{-1})	Position PA: Width	Freq. MHz
C2.6	18 May 09:18	18 May 09:35	2.00×10^{-3}	N12E61	
Peak at 09:25, SF, in AR9957 by G08 and SVI					
C3.0	18 May 10:42	18 May 12:09	1.10×10^{-2}	S14E36	
Peak at 11:39, SF, in AR9955 by G08 and RAM					
CME	18 May 11:50		614	163°(46°)	
CME Lift-off: 18 May 10:56					
CME	18 May 13:27		415	222°(144°)	
CME Lift-off: 18 May 12:18					
C2.5	18 May 12:36	18 May 12:42	8.30×10^{-4}	N12E80	
Peak at 12:39, SF, in AR9960? by G10 and SVI					
CME	18 May 16:06		789	103°(4°)	
CME Lift-off: 18 May 15:21, Only 3 points					
C3.4	18 May 15:40	18 May 15:48	1.40×10^{-3}	N11E54	
Peak at 15:44, SF, in AR9957 by G08 and HOL					
C2.2	18 May 18:24	18 May 18:33	1.00×10^{-3}	N11E53	
Peak at 18:29, SF, in AR9957 by G08 and RAM					
C1.4	18 May 21:22	18 May 21:31	6.30×10^{-4}	—	
Peak at 21:26, by G08					
C1.3	19 May 00:17	19 May 00:23	3.90×10^{-4}	—	
Peak at 00:20, by G08					
C1.4	19 May 01:38	19 May 01:49	8.00×10^{-4}	—	
Peak at 01:43, by G08					
CME	19 May 02:50			82°(8°)	
Very Poor Event					
C1.1	19 May 06:46	19 May 06:59	8.00×10^{-4}	N14E45	
Peak at 06:49, SF, in AR9957 by G08 and LEA					
C2.5	19 May 08:08	19 May 09:02	6.10×10^{-3}	—	
Peak at 08:34, by G08					
CME	19 May 08:50			90°(72°)	
Very Poor Event					
C1.4	19 May 14:07	19 May 14:12	3.80×10^{-4}	—	
Peak at 14:10, by G08					
C1.4	19 May 15:54	19 May 16:03	6.80×10^{-4}	—	
Peak at 15:58, by G08					
C2.3	19 May 16:18	19 May 16:24	6.10×10^{-4}	N08E37	
Peak at 16:22, SF, in AR9961 by G08 and HOL					
CME	19 May 18:06		448	156°(7°)	
CME Lift-off: 19 May 16:49					
C2.2	19 May 05:19	19 May 17:16	1.30×10^{-3}	S22E76	
Peak at 17:11, SF, in AR9961 by G08 and HOL					

Table 1.:Type IV_{IP} Radio Bursts and Associated Activity-Continued

Obs.	Start Universal Time	End	F_{SXR}^{tot} (J m^{-2}) V_{CME} (km s^{-1})	Position PA: Width	Freq. MHz
C2.7	19 May 18:41	19 May 18:49	1.10×10^{-03}	—	
		Peak at 18:46, by G08			
C3.1	19 May 19:09	19 May 19:19	1.30×10^{-03}	—	
		Peak at 19:14, by G08			
CME	19 May 20:26		541	225°(125°)	
		CME Lift-off: 19 May 19:45, Partial halo			
C2.1	19 May 19:46	19 May 19:54	9.20×10^{-4}	—	
		Peak at 19:50 by G08			
C2.8	19 May 20:01	19 May 20:27	3.00×10^{-3}	—	
		Peak at 20:23 by G08			
C4.7	19 May 21:43	19 May 21:52	1.90×10^{-3}	—	
		Peak at 21:48 by G08			
CME	20 May 00:50		192	41°(93°)	
		CME Lift-off: 19 May 21:43			
C2.2	20 May 07:19	20 May 07:34	1.10×10^{-3}	—	
		Peak at 07:33 by G08			
C3.9	20 May 07:29	20 May 08:14	7.60×10^{-3}	S23E74	
		Peak at 08:05, SF, in AR9961 by G08 and LEA			
CME	20 May 11:06		658	134°(38°)	
		CME Lift-off: 20 May 10:13			
M4.7	20 May 10:14	20 May 10:34		S22E76	
		Peak at 10:29, in AR9961 by G08			
M5.0	20 May 10:49	20 May 10:56		S22E76	
		Peak at 10:53, in AR9961 by G08			
CME	20 May 16:50		196	35°(91°)	
		CME Lift-off:20 May 14:12, Poor Event, C2 Only			
CME	20 May 15:50		553	143°(69°)	
		CME Lift-off: 20 May 14:45			
X2.1,	20 May 15:21	20 May 15:31	6.50×10^{-2}	S21E65	
		Peak at 15:27, 2N, in AR9961 by G08 and HOL			
C4.1	20 May 18:15	20 May 18:25	2.10×10^{-3}	S23E67	
		Peak at 18:20, 1F, in AR9961 by G08 and HOL			
C1.8	20 May 19:46	20 May 19:56	9.80×10^{-4}	S24E70	
		Peak at 19:51, SF, in AR9961 by G08 and HOL			
C3.0	20 May 20:17	20 May 20:37	3.00×10^{-3}	S21E62	
		Peak at 20:24, SF, in AR9961 by G08 and HOL			
C2.0	20 May 21:16	20 May 21:24	7.90×10^{-4}	—	
		Peak at 21:20, by G08			
CME	21 May 02:50		319	307°(26°)	
		CME Lift-off: 21 May 01:06			

Table 1.:Type IV_{IP} Radio Bursts and Associated Activity-Continued

Obs.	Start Universal Time	End	F_{SXR}^{tot} (J m^{-2}) V_{CME} (km s^{-1})	Position PA: Width	Freq. MHz
C2.2	21 May 01:39	0521 01:48	9.30×10^{-4}	S24E58	
	Peak at 01:44, SF, in AR9961 by G08 and LEA				
CME	21 May 04:26		294	314°(37°)	
	CME Lift-off: 21 May 02:50				
C4.8	21 May 04:58	21 May 05:10	2.20×10^{-3}	N15E44	
	Peak at 05:03, SF, in AR9960 by G08 and LEA				
CME	21 May 10:50		283	251°(73°)	
	CME Lift-off: 21 May 09:04				
C1.9	21 May 10:15	21 May 10:29	1.30×10^{-3}	N12E29	
	Peak at 10:21, SF, in AR9960 by G08 and SVI				
C3.2	21 May 17:17	21 May 17:30	1.80×10^{-3}	N11E69	
	Peak at 17:23, SF, in AR9963 by G08 and RAM				
CME	21 May 21:50		853	54°(135°)	
	CME Lift-off: 21 May 21:11, Partial halo				
M1.5	21 May 21:20	21 May 22:00	2.40×10^{-2}	N17E38	
	Peak at 21:39, 2F, in AR9960 by G08 and HOL				
C9.7	21 May 23:14	22 May 01:28	5.00×10^{-2}	—	
	Peak at 22 May 00:30 by G08				
CME	22 May 00:06		1246	272°(186°)	
	CME Lift-off: 21 May 23:38, Partial halo				
CME	22 May 03:50		1557	250° - halo	
	CME Lift-off: 21 May 03:15				
C5.0	22 May 03:18	22 May 05:02	2.50×10^{-2}	S22W53	
	Peak at 03:54, SF by G08 and SVI				
Type II	22 May 04:10	23 May 10:40			0.50: 0.03
	FastType II by *Wind*/WAVES				
CME	22 May 06:26		831	258°(60°)	
	CME Lift-off: 22 May 05:29				
C1.7	22 May 08:24	22 May 08:48	2.20×10^{-3}		
	Peak at 08:31, by G08				
CME	22 May 09:50		559	213°(37°)	
	CME Lift-off:22 May 09:14				
CME	22 May 12:06		444	118°(30°)	
	CME Lift-off:22 May 10:53				
C2.5	22 May 15:39	22 May 15:55	1.80×10^{-3}	S23E44	
	Peak at 15:47, SF, in AR9961 by G08 and RAM				
CME	22 May 20:26		305	16°(46°)	
	CME Lift-off:22 May 18:52				
C2.4	22 May 20:48	22 May 20:59	1.20×10^{-3}	S23E40	
	Peak at 20:54, SF, in AR9961 by G08 and HOL				

Table 1.:Type IV_{IP} Radio Bursts and Associated Activity-Continued

Obs.	Start Universal Time	End	F^{tot}_{SXR} (J m^{-2}) V_{CME} (km s^{-1})	Position PA: Width	Freq. MHz
CME	22 May 22:06		212	285°(66°)	
		CME Lift-off:Uncertain			
B9.5	23 May 01:01	23 May 01:14	6.60×10^{-4}	—	
		Peak at 01:06 by G08			
C1.1	23 May 02:30	23 May 02:43	7.70×10^{-4}	—	
		Peak at 02:35 by G08			
CME	23 May 09:50		318	228°(17°)	
		CME Lift-off:23 May 08:46			
Compact Event 35: 16 May 2002					
Type II	16 May 01:13	16 May 03:30			40: 2.0
Type IV	16 May 00:46	16 May 05:45			600: 7.0
Type II (Intermittent tone) and IV_{IP} with coronal extension by *Wind*/WAVES, CUL and LEA					
Type III	16 May 01:35	16 May 05:30			400: 1.0L
		Intermittent Activity, by *Wind*/WAVES, CUL and LEA with Largest Type III Group 0320-0500			
C 4.5	16 May 00:11	16 May 01:18	1.50×10^{-2}		
		Peak at 00:35 by G08			
CME	16 May 00:50		600	158° - halo	
		CME Lift-off:15 May 23:45			
CME(s)Preceding Main Ejection					
CME	15 May 23:06		698	88°(93°)	
CME	15 May 12:54		919	89°(95°)	
Compact Event 36: 17 April 2002					
Type II	17 Apr. 08:30	19 Apr. 04:00			5: 0.040
Type IV	17 Apr. 08:03	17 Apr. 11:50		S14W34	243: 8.0
		Type II (Intermittent bands) by *Wind*/WAVES and IV_{IP} with coronal extension by ART-4, LEA and NRH			
Type III	17 Apr. 07:51	17 Apr. 09:03			10: 1.0L
Type III Group (GG), by *Wind*/WAVES, ART-4, LEA and NRH					
M2.6	17 Apr. 07:4	17 Apr. 09:57	1.50×10^{-1}	S14W34	
		Peak at 08:24, 2N, in AR9906 by G08 and SVI			
CME	17 Apr. 08:26		1240	292° - halo	
		CME Lift-off:17 Apr. 07:50			
CME(s)Preceding Main Ejection					
CME	16 Apr. 13:50		166	290°(50°)	
CME	16 Apr. 11:06		496	262°(56°)	
CME	15 Apr. 18:06		566	240°(98°)	

Table 1.:Type IV_{IP} Radio Bursts and Associated Activity-Continued

Obs.	Start Universal Time	End	F_{SXR}^{tot} (J m^{-2}) V_{CME} (km s^{-1})	Position PA: Width	Freq. MHz
Compact Event 37: 05 October 2001					
Type II	05 Oct. 10:12	05 Oct. 11:45		S20W90	80: 1.2
Type IV	05 Oct. 10:10	05 Oct. 13:00		S20W90	100: 7.0
Type II (F-H) by *Wind*/WAVES, DAM, NRH and IV_{IP} with coronal extension by *Wind*/WAVES, DAM, NRH					
Type III	05 Oct. 10:26	05 Oct. 10:30			80: 10L
Group (GG), by *Wind*/WAVES, DAM, NRH					
C 2.5	05 Oct. 08:13	05 Oct. 08:30	2.10×10^{-3}		
Peak at 08:20 by G08					
C1.9	05 Oct. 11:31	05 Oct. 11:39	8.30×10^{-4}	S12W26	
Peak at 11:35, SF, in AR9641 by G08 and SVI					
CME	05 Oct. 10:30		1537	222° - halo	
CME Lift-off: 05 Oct. 09:56					
CME(s)Preceding Main Ejection					
CME	05 Oct. 09:30		219	235°(54°)	
Compact Event 38: 01 October 2001					
Type IV	01 Oct. 06:30	01 Oct. 07:00			4: 10
Type II	01 Oct. 07:00	01 Oct. 18:30			1: 0.15
Type IV_{IP} and Strong II (F-H) by *Wind*/WAVES					
Type II	01 Oct. 06:07	01 Oct. 07:08			90: 30
Type IV	01 Oct. 05:34	01 Oct. 08:30		S29W76	210: 10
Coronal Type II/IV by HiRAS, LEA and NRH					
Type III	01 Oct. 04:46	01 Oct. 05:20			144: 1.0L
Type III Group (GG), by *Wind*/WAVES, HiRAS, NRH					
M 9.1	01 Oct. 04:41	01 Oct. 05:23	8.60×10^{-2}	S29W76	
Peak at 05:15, in AR9628? by G10					
CME	01 Oct. 05:30		1405	225° - halo	
CME Lift-off: 01 Oct. 05:21					
CME(s)Preceding Main Ejection					
CME	01 Oct. 01:54			220°(68°)	

Table 1.:Type IV_{IP} Radio Bursts and Associated Activity-Continued

Obs.	Start Universal Time	End	F^{tot}_{SXR} (J m^{-2}) V_{CME} (km s^{-1})	Position PA: Width	Freq. MHz
Compact Event 39: 11 April 2001					
Type II	11 Apr. 13:15	11 Apr. 14:15			14: 1.50
Type IV	11 Apr. 13:15	11 Apr. 16:00			14: 9.0
	Type II (F-H) and IV_{IP} by *Wind*/WAVES				
Type II	11 Apr. 13:09				34: 25L
Type IV	11 Apr. 13:08	11 Apr. 15:19		S22W27	180H: 25L
	Coronal Type II by SVI and IV by SVI, NRH				
Type III	11 Apr. 13:01	11 Apr. 13:28			180H: 1.0L
	Type III Group (GG), by *Wind*/WAVES, SVI, NRH				
M2.3	11 Apr. 12:56	11 Apr. 13:49	4.80×10^{-2}	S22W27	
	Peak at 13:26, 1F, in AR9415 by G08 and RAM				
CME	11 Apr. 13:32		1103	224° - halo	
	CME Lift-off: 11 Apr. 12:52				
CME(s)Preceding Main Ejection					
CME	11 Apr. 06:3		858	238°(72°)	
CME	11 Apr. 00:54		939	247°(69°)	
Compact Event 40: 10 July 2000					
Type II	10 July 22:00	10 July 23:30			14: 1.0
Type IV	10 July 22:00	10 July 23:00			14: 5.0
	ComplexType II and IV_{IP} by *Wind*/WAVES				
Type II/IV	10 July 21:27	10 July 23:05			500H: 18
	Coronal Type II(F-H)/IV by CUL, HiRAS				
Type III	10 July 21:27	10 July 22:53			500H: 1.0L
	SeveralType III Groups (G–GG), by *Wind*/WAVES, CUL, HiRAS				
M5.7	10 July 21:05	10 July 22:27	2.20×10^{-1}	N18E49	
	Peak at 21:42, Peak 21:11, 2B, in AR9077 by G08 and HOL				
CME	10 July 21:50		1352	94°(289°)	
	CME Lift-off:10 July 21:12, Partial halo				
CME(s)Preceding Main Ejection					
CME	10 July 04:50		623	99°(59°)	

Table 1.:Type IV_{IP} Radio Bursts and Associated Activity-Continued

Obs.	Start Universal Time	End	F^{tot}_{SXR} (J m^{-2}) V_{CME} (km s^{-1})	Position PA: Width	Freq. MHz
Compact Event 41: 2000 June 17					
Type II	17 June 03:00	17 June 04:15			14: 1.0
Type IV	17 June 03:20	17 June 03:35			14: 7.0
Type II and IV_{IP}(Complex IV including U-bursts.), by *Wind*/WAVES					
Type IV	17 June 02:47	17 June 04:43			200H: 20L
Coronal Type IV by CUL					
Type III	17 June 02:34	17 June 04:39			200H: 1.0L
Type III Storm (S) by *Wind*/WAVES and CUL					
M3.5	17 June 02:25	17 June 02:44	2.40×10^{-2}	N22W72	
Peak at 02:37, 2B, in AR9033 by G08 and LEA					
CME	17 June 03:28		857	301°(133°)	
CME Lift-off: 17 June 02:27, Partial halo					
CME(s)Preceding Main Ejection					
CME	15 June 22:06		362	348°(102°)	
Poor Event					
Compact Event 42: 2000 May 22					
Type IV	22 May 01:30	22 May 03:30			14: 6.0
Type IV_{IP}, by *Wind*/WAVES					
Type IV	22 May 01:16	22 May 04:00D			200H: 20L
Coronal Type IV, by CUL					
Type III	22 May 01:16	22 May 01:46			200H: 1.0L
Group (GG), by *Wind*/WAVES, CUL					
C6.3	22 May 01:20	22 May 02:54	2.90×10^{-2}		
Peak at 02:01 by G08					
CME	22 May 01:50		649	245° - halo	
CME Lift-off: 22 May 00:55					
CME(s)Preceding Main Ejection					
CME	22 May 01:27		689	203°(119°)	

Table 1.:Type IV_{IP} Radio Bursts and Associated Activity-Continued

Obs.	Start Universal Time	End	F^{tot}_{SXR} (J m^{-2}) V_{CME} (km s^{-1})	Position PA: Width	Freq. MHz
Compact Event 43: 27 April 2000					
Type IV	27 Apr. 14:40	27 Apr. 14:55			14: 5.0
Possible Type IV_{IP}, by *Wind*/WAVES					
Type IV	27 Apr. 09:00	27 Apr. 15:00D		N40E00	100: 400
Coronal Type IV by ART-IV and NRH (Frequency GAP 100: 14 MHz)					
B9.4	27 Apr. 13:52	27 Apr. 13:59	3.10×10^{-4}		
Peak at 13:57 by G08					
B9.8	27 Apr. 14:04	27 Apr. 14:56	2.40×10^{-3}		
Peak at 14:40 by G08					
CME	27 Apr. 12:30		764	123°(122°)	
CME Lift-off: 27 Apr. 11:42, Uncertain Width, Partial halo					
CME	27 Apr. 14:30		1110	301°(138°)	
CME Lift-off: 27 Apr. 13:50, Partial halo					
CME(s)Preceding Main Ejection					
CME	26 Apr. 16:19		212	153°(31°)	
CME	25 Apr. 16:06		672	296°(34°)	
CME	25 Apr. 14:06		189	263°(49°)	
Compact Event 44: 11 June 1999					
Type II	11 June 11:45	11 June 17:00			14: 0.40
Type IV	11 June 11:30	11 June 12:20			14: 7.0
Type IV_{IP} and II, by *Wind*/WAVES					
Type II/IV	11 June 11:16	11 June 11:45		N30E90	35L: 300
Coronal Type II/IV by IZM, ART-IV and NRH					
Type III	11 June 11:12	11 June 12:11			500: 1.0L
Four Groups (G–GG), by *Wind*/WAVES, IZM and ART-IV					
C8.8	11 June 11:07	11 June 12:31	3.10×10^{-2}		
Peak at 11:57 by G10					
CME	11 June 11:26		1569	38°(181°)	
CME Lift-off: 11 June 11:05, Uncertain Width, Partial halo					
CME(s)Preceding Main Ejection					
CME	10 June 14:50		412	87°(115°)	
CME	10 June 11:50		215	78°(55°)	
Poor Event					

Table 1.:Type IV_{IP} Radio Bursts and Associated Activity-Continued

Obs.	Start Universal Time	End	F_{SXR}^{tot} (J m^{-2}) V_{CME} (km s^{-1})	Position PA: Width	Freq. MHz
Extended Event 45: 27–28 May 1999					
Type II/IV	27 May 10:55	28 May 15:00			14: 0.070
	Type IV_{IP} followed by II, by *Wind*/WAVES				
Type IV	27 May 10:55	27 May 15:00D		N18E31	25L: 70H
Type IV	28 May 11:30	28 May 15:00D		N18E31	25L: 70H
	Two Coronal Type IV, by SVI, DAM and NRH				
Type II	27 May 10:48	27 May 10:55			20: 55
	Type II, by DAM				
Type III	27 May 10:55	27 May 11:08			20: 70
	Type III Group (GG) , by DAM				
C1.2	27 May 09:13	27 May 09:20	4.00×10^{-4}	N31W07	
	Peak at 09:17, SF, in AR8551 by G08 and SVI				
C4.5	27 May 11:36	27 May 11:54	3.40×10^{-3}	S30E78	
	Peak at 11:43, SF, in AR8557 by G08 and RAM				
C3.4	27 May 12:59	27 May 13:09	1.60×10^{-3}	N18E31	
	Peak at 13:04, 1F, in AR8552 by G08 and HOL				
C2.7	27 May 14:23	27 May 15:05	5.90×10^{-3}	S22W76	
	Peak at 14:40, SF, in AR8548 by G08 and RAM				
C6.2	27 May 15:15	27 May 16:03	1.40×10^{-2}	S26E81	
	Peak at 15:35, SF, in AR8557 by G08 and HOL				
C7.4	27 May 16:49	27 May 17:08	7.60×10^{-3}	N38W76	
	Peak at 16:59, SF, in AR8545 by G08 and RAM				
C2.3	27 May 18:3	27 May 19:13	5.00×10^{-3}	N17E29	
	Peak at 18:59, SF, in AR8552 by G08 and COM				
C2.3	28 May 05:49	28 May 05:58	8.90×10^{-4}	N12E81	
	Peak at 05:53, SF, in AR8558 by G08 and COM				
C1.2	28 May 08:23	28 May 08:40	1.10×10^{-3}		
	Peak at 08:31 by G10				
CME	27 May 11:06		1691	341° - halo	
	CME Lift-off:27 May 10:33				
CME	27 May 14:50		646	61°(140°)	
	CME Lift-off: 27 May 13:36, Partial halo				
CME	27 May 16:26		798	116°(94°)	
	CME Lift-off: 27 May 15:23				
CME	27 May 19:27		595	46°(122°)	
	CME Lift-off: 27 May 17:41, Partial halo, 3 points				
CME	28 May 09:50		411	110°(75°)	
	CME Lift-off: 28 May 09:06				
CME	28 May 10:26		206	12°(104°)	
	CME Lift-off: 28 May 07:48				

Table 1.:Type IV_{IP} Radio Bursts and Associated Activity-Continued

Obs.	Start Universal Time	End	F_{SXR}^{tot} (J m^{-2}) V_{CME} (km s^{-1})	Position PA: Width	Freq. MHz
Compact Event 46: 03 May 1998					
Type IV	03 May 22:30	03 May 23:00			14: 8.0
		Type IV_{IP}, by *Wind*/WAVES			
M1.4	03 May 21:12	03 May 21:49	2.10×10^{-2}	N25E26	
		Peak at 21:29, in AR8214 by G09			
CME	03 May 22:03		649	302°(194°)	
		CME Lift-off: 03 May 20:58			
CME(s)Preceding Main Ejection					
CME	03 May 03:17		399	296°(22°)	
CME	02 May 14:06		938	331° - halo	
Compact Event 47: 02 May 1998					
Type II	02 May 14:25	02 May 14:50			5.0: 3.0
Type IV	02 May 14:10	02 May 15:40			14: 8.0
		Possible Type II (Narrowband wisps) and Broadband IV_{IP}, by *Wind*/WAVES			
Type II	02 May 13:30	02 May 13:46			400: 6.0
		Type II (Multiple Bands), by *Wind*/WAVES, ART-IV and DAM			
Type III	02 May 13:34	02 May 14:00			600H: 1.0L
		Group (GG) by *Wind*/WAVES, ART-IV and DAM			
Type IV	02 May 13:30	02 May 15:36		S15W15	600H: 20
		Coronal Type IV by NRH, ART-IV and DAM			
X1.1	02 May 13:31	02 May 13:51	6.70×10^{-2}	S15W15	
		Peak at 13:42, 3B, in AR8210 by G09 and RAM			
CME	02 May 14:06		938	331° - halo	
		CME Lift-off: 02 May 13:07			
CME(s)Preceding Main Ejection					
CME	02 May 05:32		542	154° - halo	
CME	01 May 23:40		585	126° - halo	
		Only C3			
Compact Event 48: 29 April 1998					
Type IV	29 Apr. 17:00	29 Apr. 18:15			14: 8.0
Type II	29 Apr. 16:30	29 Apr. 17:00			10: 2.0
		Possible Type IV_{IP} and Broadband II, by *Wind*/WAVES			
M6.8	29 Apr. 16:06	29 Apr. 16:59	1.00×10^{-1}	S18E20	
		Peak at 16:37, 3B, in AR8210 by G09 and HOL			
Type III	29 Apr. 16:06	29 Apr. 17:15			14H: 1.0L
		Group (GG) by *Wind*/WAVES, No Data above 14 MHz			
CME	29 Apr. 16:59		1374	336° - halo	
		CME Lift-off: 29 Apr. 16:22			

Table 1.:Type IV_{IP} Radio Bursts and Associated Activity-Continued

Obs.	Start Universal Time	End	F^{tot}_{SXR} (J m^{-2}) V_{CME} (km s^{-1})	Position PA: Width	Freq. MHz
CME(s)Preceding Main Ejection					
CME	27 Apr. 08:56		1385	79° - halo	